

The Role of “Live” in Livestreaming Markets: Evidence Using Orthogonal Random Forest

Ziwei Cong, Jia Liu, Puneet Manchanda¹

July 8, 2021

This version: August 17, 2022

¹Ziwei Cong is an Assistant Professor of Marketing, Georgetown University. Email: Ziwei.Cong@georgetown.edu. Jia Liu is an Assistant Professor of Marketing, Hong Kong University of Science and Technology. Email: jialiu@ust.hk. Puneet Manchanda is Isadore and Leon Winkelman Professor, Stephen M. Ross School of Business, University of Michigan. Email: pmanchan@umich.edu. The paper is part of the first author’s dissertation. The authors would like to thank Asim Ansari, Bryan Bollinger, Bruno Castelo Branco, Kinshuk Jerath, Donald Lehmann, Shijie Lu, Ralf van der Lans, Jie Zhang, and seminar participants at Georgetown University, the University of Texas at Dallas, the University of Virginia, Erasmus University Rotterdam, the University of Cambridge, the University of Chile, the University of Hong Kong, the 2022 Bass FORMS Conference, the 2021 Marketing Science Conference, the 2021 Joint Statistical Meetings & the 2020 AIML Conference for their feedback.

Abstract

A common belief about the growing medium of livestreaming is that its value lies in its “live” component. We examine this belief by comparing how the price elasticity of demand for live events varies before, on the day of, and after livestream. We do this using unique and rich data from a large livestreaming platform that allows consumers to purchase the recorded version of livestream after the stream is over. A challenge in our context is that there exist high-dimensional confounders whose relationships with treatment policy (i.e., price) and outcome of interest (i.e., demand) are complex and only partially known. We address this challenge via the use of a generalized Orthogonal Random Forest framework for heterogeneous treatment effect estimation. We find significant temporal dynamics in the price elasticity of demand over the entire event life-cycle. Specifically, demand becomes less price sensitive over time to the livestreaming day, turning to inelastic on that day. Over the post-livestream period, the demand for the recorded version is still sensitive to price, but much less than in the pre-livestream period. We further show that this temporal variation in price elasticity is driven by the quality uncertainty inherent in such events and the opportunity of real-time interaction with content creators during the livestream.

Keywords: Livestreaming, Creator Economy, Price Elasticity, Heterogeneous Treatment Effects, High-Dimensional Data, Machine Learning

INTRODUCTION

Livestreaming is the practice of streaming online content for consumption in real time. Compared to recorded content, the key benefits of livestreaming are its immediacy, authenticity, and opportunity of audience-streamer interaction during the stream (Hu, Zhang, and Wang 2017; Lin, Yao, and Chen 2021). These attributes have made livestreaming a big and growing phenomenon worldwide, e.g., the livestreaming industry is valued at \$16.3 billion in China (Statista 2020), and \$11 billion in the U.S. (Thomas and Palmer 2021). Twitch, the leading U.S. livestreaming platform for gaming, has seen monthly audiences growing at 300% in the 2015-18 period (Iqbal 2021). Social media platforms, such as Facebook, have launched livestream functions so that users can monetize followers via hosting paid events. E-commerce giants (e.g., Alibaba and Amazon) and many brands (e.g., Walmart, Macy's, Avon, LG, Nordstrom, and Petco) have fully embraced livestreaming selling and promotion (Larson 2021; Wheless 2021). Therefore, it is increasingly important for content creators, platforms and marketers to understand the economic value created by livestreaming.

A common belief about the growing medium of livestreaming is that its value lies in its “live” component. Thus, many livestreaming platforms (e.g., Instagram Live, Wechat Live, and YouNow) only support live broadcasts and do not offer built-in recording functions. Other platforms, such as Facebook Live and Periscope, offer built-in recording and replay functions, but devote very limited resources towards the management and marketing of recorded versions of live events. Due to the novelty of livestreaming, however, no research has compared consumer purchase behavior of live-streamed and recorded content. This paper aims to fill in this research gap using data from one of the largest livestreaming platforms in China, Zhihu Live. We leverage the fact that the platform also makes the recorded version of live content available for purchase at the same price, allowing us contrast consumer responses to the content (i.e., demand and price elasticity of demand) before, on the day of, and after the livestream.

Zhihu Live targets creators who want to monetize their expertise or establish their own business

via livestreaming. Creators on Zhihu Live can launch paid live events (denoted as “Live” in the rest of the paper) on specific topics, such as cooking, culture, business, etc. A Live is usually listed on the market for purchase 2-3 weeks prior to its scheduled airing day. During the livestream, creators give a 1-2 hour live talk and interact with a paid audience in a virtual chat room. After the livestream concludes, its recorded version is available for purchase at the same price, but without the opportunity of creator-audience real-time interaction. Zhihu Live uses the most common pricing model in livestreaming markets — pay-per-view — that is also used by Facebook, Vimeo, OnlyFans, etc. Each creator sets a common price for her/his live and recorded content with consumers paying this fixed price one time.¹

An ideal way to estimate the price elasticity of demand is using randomized field experiment. But randomization is difficult in our context due to the non-standardized, one-off nature of user-generated live content in online social networks. This makes observational data the primary source for demand estimation, which is still challenging for two major reasons. First, prices and demand are likely to be confounded with a large number of factors (e.g., content quality and creator credibility). For example, creators may anticipate demand based on own reputation in the Q&A community and set price accordingly. More importantly, the confounding factors often influence price and demand in potentially complex and partially known ways. In other words, the number of potential covariates formed by transforms and/or interactions of these confounders can be very large. This can result in a situation where the number of model parameters is large relative to the sample size. Second, the price elasticity for such products is likely to be heterogeneous, both across Lives and over the event life-cycle. Given the novelty of this type of markets and products, we have little prior knowledge on the potential patterns of heterogeneity in price elasticity. Therefore, conventional parametric approaches for exploring heterogeneity can be restrictive in this context.

To address the above challenges, we adopt a framework that allows us to estimate the price

¹In livestreaming, pay-per-view is considered to be a “direct” pricing model mechanism, along with subscriptions, and pay-what-you-want (PWYW) or tipping (Lu et al. 2021; Lin, Yao, and Chen 2021). Some platforms follow an “indirect” pricing model, i.e., revenue is generated via ad and/or product placement during the livestream.

elasticity of demand non-parametrically in the presence of high-dimensional confounders whose relationships with demand are complex and partially known. Specifically, our framework generalizes Orthogonal Random Forest (ORF) (Oprescu, Syrgkanis, and Wu 2018) via the use of semi-parametric Deep Neural Networks (SDNNs) to estimate nuisance functions (i.e., functions of all confounding variables). SDNNs allow partitioning of confounders into two sets. The first set of confounders are assumed to have known relationships with the treatment and outcome variables, while the second set are assumed to have unknown relationships with the treatment and outcome variables. Such a semi-parametric approach is particularly suited to marketing and economics settings (e.g., when panel data are used) because the method allows for “fixed effects” while accommodating flexible non-linear combinations of the remaining confounders. As a result, researchers can apply their pre-existing knowledge to specify the functional forms of some covariates in the nuisance functions, while automating the search for relevant functional forms for the other covariates. In this way, researchers do not need to make strong assumptions on which and how all of the covariates influence the treatment or outcome variables.

Our estimation results show significant dynamics in price elasticity over the Live life-cycle. Demand becomes less price sensitive over time as the number of days to the Live gets smaller. On the day of the Live, demand becomes inelastic. Over the post Live period, demand for the recorded versions becomes price sensitive again, but overall it is less price sensitive than demand for the live versions. The pricing literature often assumes that high price sensitivity co-occurs with low utility (i.e., low valuation or low willingness to pay) and low price sensitivity co-occurs with high utility (i.e., high valuation or high willingness to pay). Therefore, our finding that demand is inelastic only on the day of the Live confirms that consumers indeed value the live format. More importantly, our results show that consumers also value the recorded versions of live content. We further show that this temporal variation in price elasticity is driven by the quality uncertainty inherent in such events as well as the ability to interact with creators in real-time during the livestream.

This paper makes several contributions. First, it is one of the early studies that investigate the growing phenomenon of livestreaming. While previous literature has studied the consumption of

conventional live programming like sports events on television (e.g., Vosgerau, Wertenbroch, and Carmon 2006), livestreaming by individual creators on digital platforms is still under-explored. Second, we document that, contrary to the conventional belief, the value of such livestreams is not just restricted to the live component. In our setting, the consumer willingness-to-pay for the post-livestream content is high (based on the estimated price elasticity), and the post-livestream demand accounts for 22% of total sales. Third, we show that the consumer willingness-to-pay for both live and recorded content is related to the changes in uncertainty about the quality of the experience. Fourth, we provide guidelines for offering and managing live and recorded content, especially in terms of pricing, for both platforms and creators. Finally, we extend state-of-the-art methods via the incorporation of semi-parametric approaches in the estimation of nuisance functions in ORF.

The rest of the paper is organized as follows. We first detail our empirical context and data, followed by descriptive data analyses. Next, we introduce the model setup and the algorithm, showing how SDNNs (for nuisance estimation) are incorporated into ORF. We then report our main findings as well the underlying mechanisms. Finally, we discuss the managerial implications of our findings and conclude with directions for future research.

RESEARCH CONTEXT AND DATA

Zhihu Live

Zhihu (NYSE: ZH) is the earliest and largest knowledge sharing platform in China, starting as a Q&A community (similar to Quora.com) in 2011. The latest statistics show that Zhihu has over 43.1 million cumulative content creators and over 315.3 million Q&As (CIW Team 2021). Users on the Q&A community can voluntarily seek and share information (such as knowledge, expertise, and customized solutions) in a variety of domains mainly through posting questions and answers. Users can also organically follow any other users. Each user has a profile page, which contains some personal information provided by the user and a summary of the user's past content contribution activities. We provide sample Zhihu interfaces in Appendix A.

Zhihu launched Zhihu Live on May 14, 2016, targeting creators who want to monetize their

expertise via livestreaming content to a paying audience. By December 2020, Zhihu Live had nearly 10,000 paid Lives, 5,000 unique creators and 6 million paying users (Fergus 2020). To become Live creators, users need to provide Zhihu with basic personal information, such as real name, educational background, and the proof of expertise in certain area(s). Upon approval, users are allowed to host own Lives. The revenue from Lives is split between creators and the platform — this split was 70/30 during the period of our data.

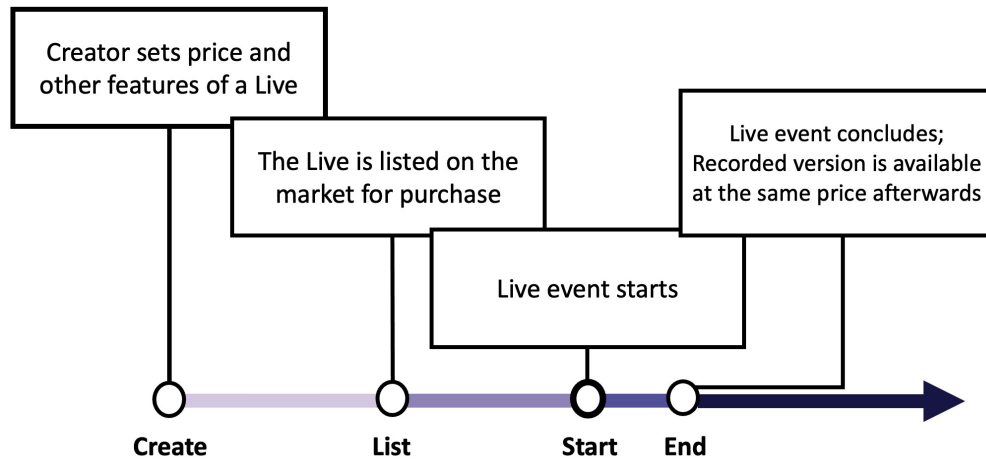


Figure 1: Life-Cycle of a Live

Figure 1 illustrates the life-cycle of a typical Live on Zhihu. A creator first decides a few key features, including full price, topic, content, starting time, and seat limit. The price is set within the range of 0.01 RMB to 499.9 RMB under loose guidance from the platform. All Live topics must fall under a set of 17 topics provided by Zhihu.² The seat limit represents the maximum number of viewers who are allowed to interact (ask questions, leave comments, etc.) with the creator during the livestream. Most creators set the seat limit to be 500. Upon approval from Zhihu, the Live is listed on the platform for purchase, typically 2-3 weeks prior to its starting time. Consumers are informed about whether seats are available when clicking into the “Purchase This Event” button. Although only the cumulative sales number is explicitly displayed on the page of

²These are Architecture & Design, Art History & Appreciation, Business, Careers, Economics & Finance, Education, Food & Cuisine, Healthcare, Internet, Law, Lifestyle, Music & Games & Movies, Psychology, Reading & Writing, Science & Technology, Sports, and Travel.

each Live, given that most of the time the seat limit is 500, consumers can infer the number of remaining seats. During the livestream, the creator gives a live talk on the topic, typically for a duration between one and two hours. The creator can interact with the audience via text, voice, or picture messages in a virtual chat room during the Live (see an example in Appendix A for a typical interaction). Note that because of the seat limit, consumers who purchase a Live after the seat limit is reached can only view the live event in a non-interactive manner. After the livestream concludes, consumers are allowed to provide feedback, i.e., a rating on a 5-point scale along with text comments. The recording of the livestream is then made available for purchase at the same price, but without the opportunity of creator-viewer real-time interaction. Consumers can search and explore all recorded Lives via a link on the Live market website.

It is important to note that once a creator sets a price for her/his Live and the Live is listed on Zhihu, the creator cannot change the price. This prevents strategic price adjustment by the creator in response to realized demand. The only possible change to the price comes from the *platform* which chooses a small set of Lives (about 15%) to promote via a discount. The platform makes the discount available to consumers sometime between the listing of the Live and the day of the livestream. As a result, creators have no influence on the choice to promote as well as the duration of the promotion. In addition, the platform runs in-site banner advertising for few Lives hosted by celebrities. These are the only marketing activities conducted by the platform within our study period.³

Data

Our study uses two internal datasets from Zhihu. The first comprises transaction records of Live events from May 2016 to June 2017. In this part, we observe buyer ID, purchase time, unit price paid along with a rich set of characteristics describing the purchased Live. We also observe advertising and promotions of Lives run by the platform. The second data set contains all of the users

³Anecdotal evidence suggests that some creators promote their Lives on social media platforms such as Wechat and Sina Weibo, but we find that only less than 1% of all of the ticket sales originated from outside Zhihu over our study period. This suggests that this type of marketing efforts led by creators is unlikely to influence demand.

on Zhihu's Q&A community along with their historic activities. These activities include registration time (on Zhihu), content contribution, content subscription, social activities and the number of different types of feedback that users received for their contributed answers. As a result, we have access to detailed information on each creator and customer (as creators/customers need to be registered on Zhihu in order to host/buy a Live).

Our empirical study focuses on 2,705 Lives that were hosted by 1,330 creators from November 2016 to June 2017. During this period, there was no structural or policy change on the operation of the Zhihu Live market, with two exceptions which are related to the review and rating system. We describe them below and explicitly control for them in our analysis. As our goal is to estimate the temporal variation in price elasticity over the Live life-cycle, we aggregate individual transactions on each day to obtain the daily ticket sales and price of each Live.⁴ We find that approximately 90% of the sales transactions occur from the listing day to 30 days after the livestream. Hence, we restrict our analysis to this window. This results in a total of 125,028 Live-day observations.

We observe rich characteristics of all relevant actors/events in this ecosystem and organize these variables into four categories in Table 1. The first category is Lives. We summarize Live attributes via variables such as topic category, seat limit, when the event was listed and aired. We also observe time-varying Live-specific variables that may influence demand over time, such as temporal distance to the airing day of the Live, cumulative demand till the current day and in-site banner advertising run by the platform (which was done for few Lives hosted by celebrities). The second category pertains to creators. Examples of creator attributes include creator's social network on Zhihu (e.g., the number of followers and of followees), content related activities in the Q&A community and experience with the Live market (e.g., the number of Lives held previously). All these are defined as cumulative counts up to the starting time of each Live. The third category pertains to the Zhihu Live market. The variables include market size, competition among Lives, topic category and the aforementioned two changes to the rating and review system. Note that

⁴Due to the sparsity of sales data per Live, we are not able to conduct analysis at a level that is finer than at the daily level. The daily ticket price of each Live is the average unit price across all tickets sold on a day. If no transactions occurred on the day, we impute the daily ticket price with the Live's regular price.

Table 1: Control Variables

Live-Specific Characteristics

- Fixed variables: The num. of days from listing to livestream; Seat limit; Rating; Whether livestream is held on public holiday; *Topic indicators*; *livestream week indicators*; *livestream day-of-week indicators*
- Time-varying variables: The cum. sales of a Live; Whether seats are still available; Whether the Live is advertised by the platform; Percentage discount; *Temporal distance relative to livestream indicators*

Creator-Specific Characteristics

- Social network: The cum. num. of followers/followees
- Content contribution in the Q&A community: The cum. num. of answers/questions/articles; The cum. num. of up-votes/down-votes/thank/unhelpful that own posted answers received
- Past Live experience: The cum. num. of hosted Lives; The average sales of past Lives; The average rating of past Lives; The average num. of reviews of past Lives; The average num. of “likes” of past Lives; The num. of days since the first Live
- Profile: The num. of days since registered Zhihu; Whether is a off-line celebrity; Whether is invited to open Live; Whether is an “Excellent Contributor” certified by Zhihu;
- *Creator indicators*

Market-Level Factors

- Market size: The num. of days since launching Zhihu Live; The cum. num. of (unique) consumers/creators/Lives on the market; The num. of running Lives on the same day
- Competition: The cum. num. of available Lives from the same topic; The num. of running Lives from the same topic on the same day; The average price of available Lives from the same topic; The average price of running Lives from the same topic on the same day; The average follower size of other Live’ creators from the same topic; The average follower size of other creators who running Lives in the same topic on the same day
- Policy change: Whether Live rating function was launched (November 02, 2016); Whether detailed reviews were displayed to public (April 24, 2017)

Platform-Level Factors

- User base: The cum. num. of users; The daily num. of newly registered users
 - Voluntary content contribution: The cum. num. of questions/answers; The daily number of newly posted questions/answers
 - Seasonal/Temporal shocks: *calendar week indicators*; *day-of-week indicators*
-

during the period of our data, Zhihu Live was the leading platform of its type in China, i.e., across-platform competition was not a factor in influencing demand and/or prices.⁵ The fourth category pertains to the Zhihu Q&A platform. The variables here include the user base and the volume

⁵Industry reports at that time note that Zhihu Live was seen as a unique platform, leading to it be in a virtual monopoly in China in this space. See, for example, <https://zhuanlan.zhihu.com/p/311125086>.

of contributed questions and answers. Note that in our later model specifications, we capture unobserved time-invariant heterogeneity among creators via the use of creator fixed effects, and also capture temporal shocks that could affect the platform via the use of calendar week and day of the week fixed effects.

These result in a total of 1,700 control variables for estimating the price elasticity of demand for Lives. In principle, these variables are likely components of creators' strategic pricing and platform's discount policy. For example, creators may anticipate demand based on their own reputation in the Q&A community and/or competition levels in the Live market and set price accordingly. Therefore, it is important to control for these variables when estimating price elasticity, in order to address potential sources of endogeneity in the price-demand relationship. However, we have limited prior knowledge on the exact functional form that can capture how these confounding variables impact price and demand. As a result, we are faced with a large set of potential variables formed by complex transforms and/or interactions of these variables. This can potentially result in a situation where the number of model parameters is large relative to sample size.

DESCRIPTIVE ANALYSIS

In this section, we first show the relevant data patterns on creators and Lives. Then, we carry out descriptive analyses of demand and pricing to understand the data generating process and to guide the specification of our model.

Summary Statistics

Table 2 reports summary statistics of the creators observed in our study period. On average, each creator held two Lives and 60% of the creators only held one Live. Across creators, we find a large variation in experience, activity level, and reputation.⁶ Table 3 presents summary statistics of the Lives. The mean price is 22 RMB (about 3 USD), the mean seat limit is 498 (note that 95% of Lives have a seat limit of exactly 500), and the mean listing time is 17 days prior to the event.

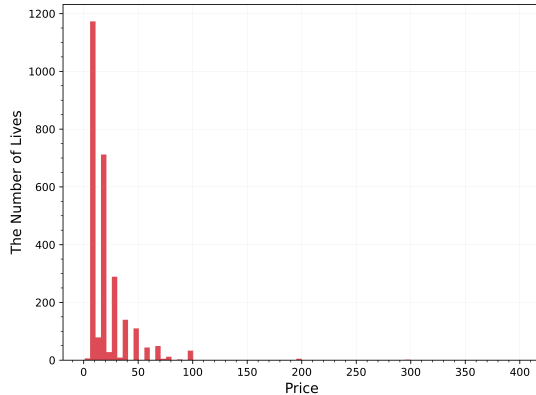
⁶For 527 creators who held more than one Live over our study period, we report the average across held Lives.

The price varies widely across Lives, ranging from 0.99 RMB to 399 RMB (see Figure 2a for the distribution of price). The mean total sales of a Live in our data set is 639, which is greater than the mean seat limit. A surprisingly high proportion, 12%, of total sales occur within 30 days *after* the livestream.

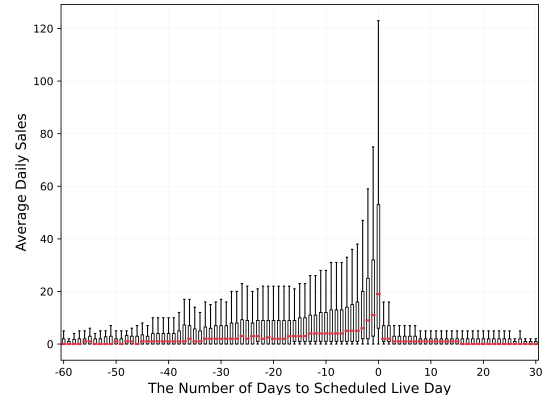
Table 3: Live Summary Statistics

Variable	Mean	Std.	Correlation						
			V1	V2	V3	V4	V5	V6	
V1 Num. Days before Livestream	17	13	1						
V2 Seat Limit	498	139	<i>0.074</i>	1					
V3 Price	22	22	<i>0.123</i>	-0.025	1				
V4 Total Sales	639	2,311	0.004	-0.021	0.018	1			
V5 Pre-livestream Sales	499	2,084	0.007	-0.018	<i>0.035</i>	<i>0.990</i>	1		
V6 30-day Post-livestream Sales	75	195	-0.015	-0.017	<i>-0.012</i>	<i>0.557</i>	<i>0.448</i>	1	

Note: The correlations in italics are statistically significant at $p < 0.1$.



(a) Distribution of Price Across Lives



(b) Average Daily Sales over Live Life-Cycle

Figure 2: Distribution of Price and Daily Sales

Figure 2b depicts the distribution of daily sales across all Lives over the Live life-cycle using a box-and-whisker plot. The box extends from the Q1 to Q3 quartile values of daily sales, with a red line at the median (Q2).⁷ As can be seen from the figure, daily ticket sales increase gradually

⁷As is typical of box-and-whisker plots, in order to enhance the visual clarity of the plot, the length of the whisker (the

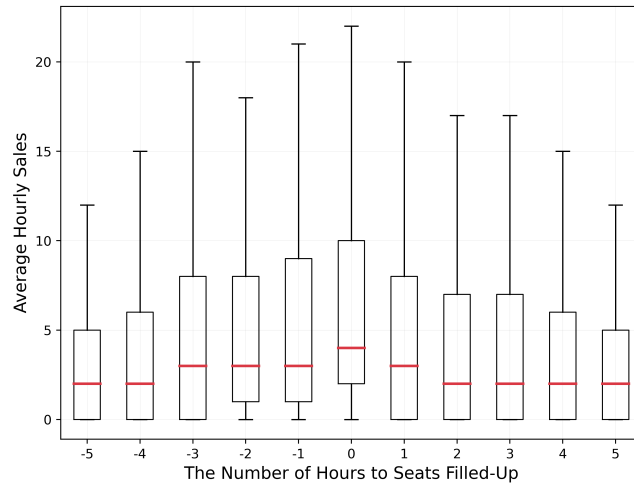


Figure 3: Average Hourly Sales over Time to Seats-Sell-Out

Note: This figure is based on 538 Lives whose seats were filled up before livestreaming day.

throughout the pre-livestream period, peak on the livestreaming day, and drop immediately afterwards. This shows that there is considerable variation in demand over the life-cycle of a typical Live.

Recall that a consumer who purchases a Live after its seat limit has been reached will no longer have the opportunity to interact with the creator during the livestream. If real-time interaction is important to consumers, we expect that demand will drop significantly after the seat limit is reached. In our data, there are 583 Lives (out of 2,705) whose seats were filled up before the livestreaming day. Figure 3 depicts the distribution of hourly sales of these Lives five hours before to five hours after the seat limit was reached using a box-and-whisker plot. One can see that the increasing time trend becomes a decreasing one immediately after the seats are filled up. This pattern is consistent with our conjecture that the opportunity of interacting with creators during livestream is important for consumers.

vertical line) is truncated at a maximum of 1.5 times the interquartile range (i.e., $Q3 - Q1$). However, we retain all data points in our empirical analyses.

Regression Analysis of Demand

In order to understand what drives consumer demand, we carry out a cross-sectional regression analysis.⁸ Our dependent variable is the log-transformed total sales of a Live in either the pre- or the post-livestream period. The independent variables include the log-transformed price and a subset of covariates shown in Table 1. This allows us to interpret the price coefficient as the price elasticity of demand. The other continuous independent variables are all standardized. For post-livestream demand, we also control for consumer ratings and log-transformed pre-livestream demand.

The full estimation results are shown in Table 4. We highlight two key findings. First, the price elasticity of pre-livestream demand (Model (1)) is significantly negative ($p < 0.01$), whereas the price elasticity of post-livestream demand (Model (2)) is not significantly different from zero. This suggests that post-livestream demand is less price sensitive than that of pre-livestream demand. Second, as expected, we find that the creator’s past experience and reputation appear to have much larger effects on pre-livestream demand than on post-livestream demand. This is probably because when Live-specific ratings become available after livestream, consumers are less likely to leverage other information cues to make purchase decisions for recorded versions.

Regression Analysis of Price

We use a cross-sectional regression analysis to understand the factors that may influence the prices set by creators. We regress the log-transformed price p_{ij} of Live j hosted by creator i on a subset of the covariates listed in Table 1. All of the continuous independent variables are standardized and hence their coefficients are comparable. The full estimation results are presented in Table 5. The estimated coefficients for Live-specific characteristics suggest that creators tend to set a lower price if the Live is to be aired on holidays ($p < 0.1$) or has fewer days on the market prior

⁸Note that we do not control for creator fixed effects in all cross-sectional regression analyses because 60% creators only held one Live in our study period. We also conduct a similar regression analysis of demand using panel data with “Live-day” as the unit of analysis. We find that results are consistent with the results from the cross-sectional regression. Details are available from the authors upon request.

Table 4: Regression of Log-Transformed Demand

Model	Pre-Livestream Period (1)	Post-Livestream Period (2)
<i>Live-Specific Features and Seasonality on Livestreaming Day</i>		
Log Price	−0.718 (0.043) ^{***}	−0.039 (0.031)
Seat Limit	−0.007 (0.023)	−0.029 (0.016) [*]
Days before Live	0.200 (0.025) ^{***}	−0.134 (0.017) ^{***}
Advertised	1.237 (0.093) ^{***}	−0.396 (0.066) ^{***}
Topic Fixed Effects	Yes	Yes
Log Pre-Livestream Demand		0.805 (0.014) ^{***}
Rating		0.167 (0.027) ^{***}
Holiday	−0.366 (0.128) ^{***}	−0.105 (0.088)
Live Day of Week Fixed Effects	Yes	Yes
Live Week Fixed Effects	Yes	Yes
<i>Creator Experience and Reputation in Live Market</i>		
Live Market Lifetime	0.051 (0.046)	−0.106 (0.032) ^{***}
Invited Creator	0.108 (0.110)	0.117 (0.075)
Num. Past Lives	−0.256 (0.039) ^{***}	0.081 (0.027) ^{***}
Average Past Pre-Livestream Demand	0.118 (0.025) ^{***}	−0.011 (0.017)
Average Past Live Rating	0.066 (0.014) ^{**}	0.027 (0.021)
<i>Creator Experience and Reputation in Q&A Community</i>		
Q&A Platform Lifetime	0.079 (0.027) ^{***}	0.043 (0.019) ^{**}
Celebrity	0.859 (0.168) ^{***}	−0.459 (0.116) ^{***}
Excellent Contributor	−0.104 (0.072)	−0.077 (0.049)
Num. Followers	0.183 (0.035) ^{***}	0.016 (0.024)
Num. Followees	0.024 (0.025)	−0.010 (0.017)
Num. Articles	0.129 (0.035) ^{***}	−0.006 (0.024)
Num. Questions	−0.200 (0.036) ^{***}	0.014 (0.025)
Num. Answers	0.062 (0.032) [*]	−0.019 (0.022)
Num. Upvotes per Ans.	0.247 (0.068) ^{***}	0.207 (0.047) ^{***}
Num. Downvotes per Ans.	0.153 (0.051) ^{***}	0.027 (0.035)
Num. Thanks per Ans.	0.033 (0.084)	−0.039 (0.057)
Num. Unhelpful per Ans.	−0.277 (0.097) ^{***}	−0.138 (0.067) ^{**}
Num. Obs.	2,705	2,705
R ²	0.483	0.716

Note: ^{***} $p < 0.01$, ^{**} $p < 0.05$, ^{*} $p < 0.1$.

to airing ($p < 0.01$). As expected, we find that creators' levels of experience or reputation — measured via the number of past Lives, the average rating of past Lives, the number of contributed questions/answers, and the number of followers on the Q&A platform — are positively associated with price level ($p < 0.01$). Similarly, we find that offline celebrities or invited creators are more likely to set higher prices.

Table 5: Regression of Log-Transformed Full Price

Model	(1)	(2)	(3)	(4)
<i>Live-Specific Features and Seasonality on Livestreaming Day</i>				
Seat Limit	-0.004 (0.011)	-0.002 (0.011)	-0.001 (0.011)	-0.001 (0.011)
Days before Livestream	0.096 (0.011)***	0.099 (0.011)***	0.065 (0.011)***	0.070 (0.011)***
Advertised		-0.087 (0.041)**	-0.066 (0.040)	-0.128 (0.042)***
Topic Fixed Effects		Yes	Yes	Yes
Holiday	-0.130 (0.061)**	-0.130 (0.061)**	-0.134 (0.059)**	-0.121 (0.058)**
Live Day of Week Fixed Effects	Yes	Yes	Yes	Yes
Live Week Fixed Effects	Yes	Yes	Yes	Yes
<i>Creator Experience and Reputation in Live Market</i>				
Live Market Lifetime			-0.049 (0.020)**	-0.033 (0.021)
Invited Creator			0.112 (0.050)**	0.134 (0.050)***
Num. Past Lives			0.131 (0.017)***	0.075 (0.018)***
Average Past Pre-Livestream Demand			-0.008 (0.011)	-0.019 (0.011)*
Average Past Live Rating			0.034 (0.014)**	0.046 (0.014)***
<i>Q&A Platform Lifetime</i>				
Offline Celebrity				-0.015 (0.012)
Excellent Contributor				0.379 (0.077)***
Num. Followers				0.023 (0.033)
Num. Followees				0.036 (0.016)**
Num. Articles				-0.016 (0.012)
Num. Questions				0.061 (0.016)***
Num. Answers				0.039 (0.017)**
Num. Upvotes per Ans.				-0.029 (0.015)*
Num. Downvotes per Ans.				-0.063 (0.031)**
Thank Num. per Ans.				0.028 (0.023)
Num. Unhelpfuls per Ans.				0.059 (0.038)
Num. Obs.	2,705	2,705	2,705	2,705
R ²	0.085	0.122	0.164	0.194

Note: *** $p < 0.01$, ** $p < 0.05$, * $p < 0.1$.

These findings suggest that, when setting prices, creators consider timing, their experience and reputation in both the paid market and the free Q&A community. This is also supported by the improvement in R^2 across different model specifications. Live specific features and seasonality together account for about 12.2% of price variation (Model (2)), while creator-specific variables account for another 7.2% of price variation (Model (4)). Note that all of the variables (included as individual regressors) account for only 19.4% of the variation in price (Model (4)). This confirms the importance of using a flexible functional form, that allows different ways of interacting and transforming these variables, for improving the explanatory power of these variables.

MODELING APPROACH

We describe our methodological approach in this section. We use our empirical context to motivate the notation for clarity of exposition, noting that it can be easily generalized to other contexts.

The Problem Setup

Let $Y_{it} \in \mathcal{R}$ denote the number of sales of Live i on day t , which is represented as a function of its treatment (i.e., price) on day t , denoted by T_{it} . We let $W_{it} \in \mathcal{R}^p$ represent a multitude of control/confounding variables, and $X_{it} \in \mathcal{R}^d$ be the feature vector that captures the heterogeneity in price elasticity. The outcome and treatment are assumed to follow a general specification as in [Oprescu, Syrgkanis, and Wu \(2018\)](#):

$$\begin{aligned} Y_{it} &= \theta_0(X_{it})T_{it} + f_0(X_{it}, W_{it}) + \varepsilon_{it} \\ T_{it} &= g_0(X_{it}, W_{it}) + \eta_{it} \end{aligned} \tag{1}$$

where ε_{it} and η_{it} represent the unobserved noise such that $\mathbb{E}[\varepsilon_{it} | T_{it}, X_{it}, W_{it}] = 0$ and $\mathbb{E}[\eta_{it} | X_{it}, W_{it}] = 0$. Note that the full set of confounding factors consists of W and X . We differentiate between the target feature and other controls using notation X as we are interested in how the treatment effect (i.e., the price elasticity), denoted as θ_0 , evolves along the target feature X . The second equation keeps track of the confounding, namely the dependence of the treatment variable on controls. The

confounding factors affect the treatment variable T via the nuisance function g_0 and influence the outcome Y via the nuisance function f_0 (Chernozhukov et al. 2018). Our goal is to estimate the conditional average treatment effect $\theta_0(x)$ conditioned on some test points x , i.e., a set of specific values on the target feature X .

Methodological Background

We now review two streams of research at the intersection of causal inference and machine learning that have been used to estimate (heterogeneous) treatment effects with observational data. The first stream of research has demonstrated the potential for the use of machine learning methods in partialing out the influence of high-dimensional potential controls. One approach in this stream is Double Machine Learning (DML) introduced in Chernozhukov et al. (2017a, 2018). DML requires first-stage estimation of both treatment and outcome functions of the high-dimensional controls. These can be done using arbitrary machine learning methods such as lasso, random forests, neural nets. Using sample splitting, the out-of-sample residuals from these models represent exogenous variation that can be used to identify a valid causal effect in a second stage regression. A challenge with this approach is that it handles heterogeneity in the treatment effect in a fairly limited manner, typically via pre-specified parametric distributions (Chernozhukov et al. 2017b).

The second stream uses random forests (and its variants) to obtain causal heterogeneous treatment effects. The most prevalent algorithm in this stream is the Generalized Random Forest (GRF) proposed by Athey, Tibshirani, and Wager (2019). GRF assigns each observation a similarity weight derived from the fraction of trees in which an observation appears in the same leaf as the target feature point. It then solves the local estimation equation using the weighted set of “neighbors” at the particular value of target feature. Therefore, GRF allows for fully flexible non-parametric estimation of heterogeneity in the treatment effect (Wager and Athey 2018; Athey, Tibshirani, and Wager 2019). This makes it particularly helpful under situations when the potential patterns of treatment heterogeneity are unknown or highly complex. However, these methods tend to perform poorly in the presence of high-dimensional or “highly complex” controls arising from the required

regularization bias — see Chernozhukov et al. (2018) for details.

ORF leverages the benefits of both DML and GRF. It allows non-parametric estimation of the target parameter while permitting more complex nuisance functions with high-dimensional parameterizations (Oprescu, Syrgkanis, and Wu 2018). At a high level, ORF incorporates DML into GRF by orthogonalizing the effect from high-dimensional controls via local two-stage estimation. In another words, ORF follows the residualization approach similar to DML to create an orthogonal moment for identifying $\theta_0(x)$ at each target point x .⁹ Importantly, ORF estimates are shown to be asymptotically normal and hence have theoretical properties that render bootstrap based confidence intervals asymptotically valid.

To illustrate the basic idea of ORF, we define a function $q_0(X, W) = \mathbf{E}[Y|X, W]$ for the problem introduced previously. We define the residuals as $\tilde{Y} = Y - q_0(X, W)$ and $\tilde{T} = T - g_0(X, W)$. Then, one can simplify the equation as $\tilde{Y} = \theta_0(X)\tilde{T} + \varepsilon$, which leads to $\mathbf{E}[\tilde{Y}|X, \tilde{T}] = \theta_0(X)\tilde{T}$. This relationship suggests that one can obtain an estimate of $\theta_0(x)$ by regressing \tilde{Y} on \tilde{T} locally around $X = x$. ORF achieves such an estimation, following the approach of GRF. Specifically, using a forest-based kernel learner, ORF first assigns a set of similarity weights between each sample and the target point x , and then computes $\hat{\theta}$ via kernel regression with the set of weights. We summarize all of the essential steps of ORF algorithm in Web Appendix A, along with the pseudo code.

The key causal identification requirement underlying all of these methods (DML, GRF and ORF) is the unconfoundedness assumption. This states that all of the variables affecting both the treatment T and the outcome Y are observed and can be controlled for. In other words, all of the confounding variables must be known and be included in (X, W) . The unconfoundedness assumption also suggests that the specification of the nuisance functions, g_0 and f_0 , is very important in making sure that all of the confounding factors are properly controlled for. The existing literature primarily uses lasso to model the nuisance functions. Lasso helps maintain interpretability, but

⁹Notably, Athey, Tibshirani, and Wager (2019) also recommend a residualization step in their empirical evaluation, which they referred to as “local centering.” The key difference between GRF “local centering” and ORF is that ORF residualizes locally around test point x , as opposed to performing an overall residualization step and then calling the GRF algorithm on the residuals. Oprescu, Syrgkanis, and Wu (2018) have shown that ORF can improve the final performance of the treatment effect estimates because residualizing locally is more appropriate than running a global nuisance estimation, which would typically minimize a non-local mean squared error.

assumes a linear relationship between covariates and outcome/treatment. This could be seen as a very restrictive formulation in the sense that non-linear relationships are ruled out a priori. On the other extreme, purely nonparametric methods such as random forests or deep neural networks (DNNs) can be used to improve flexibility and fitting, but they are not interpretable and may also lead to over-fitting issues. In the next section, we describe how we combine the best aspects of both approaches in our setting via the use of SDNNs.

SDNNs for Nuisance Estimation

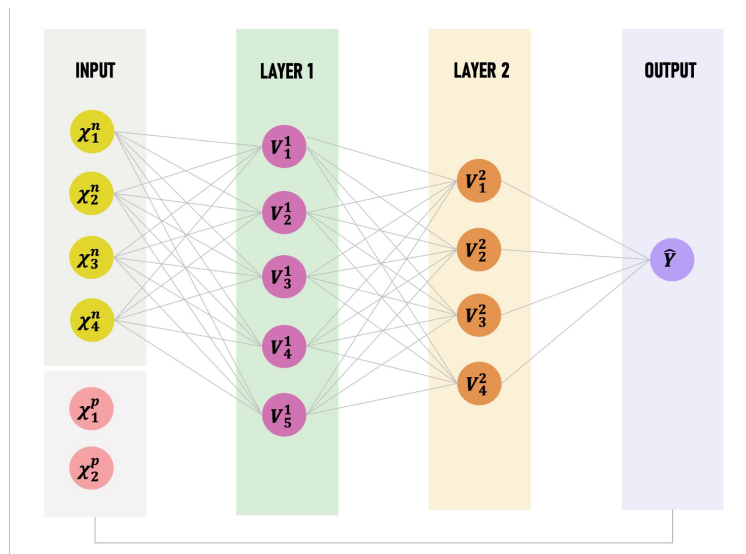


Figure 4: Semi-Parametric Neural Network Model

Note: The upper part of input is the nonparametric component, going through nonlinear transformation. The lower part of input is the parametric component, having linear relationship with the target variable.

SDNNs combine a parametric form for some known covariates (usually based on prior knowledge about data-generating process or standard econometric techniques) with flexible nonparametric forms for the remaining covariates. The basic idea of SDNNs is illustrated by a network diagram in Figure 4. SDNNs allow partitioning of the covariates into two sets. The first set consists of covariates that are assumed to have known relationships with the treatment and outcome while the second set consists of covariates that are assumed to have unknown relationships with the treatment and outcome. SDNNs are thus well-suited to settings where treatment and outcome are confounded

with many observable factors in complex but partially known ways. For example, in panel data settings, they can deal with clustering via fixed effects in a linear fashion, while accommodating non-linear combinations of the remaining covariates in a totally flexible manner (Crane-Droesch 2017; Athey and Wager 2019). An empirical comparison of SDNNs relative to other methods (i.e., lasso and standard DNNs) is provided in Web Appendix C.1. To the best of our knowledge, this paper is the first to enable SDNNs in ORF.

We operationalize SDNNs using a deep feedforward neural network architecture with multiple inputs. For ease of notation, let $\chi = (X, W)$ represent all of the observed covariates. We form two sets based on χ , denoted as χ^p and χ^n , which enter the parametric and nonparametric components of the nuisance functions, respectively. Then, we can re-write the nuisance functions as

$$q_0(\chi) = q_{01}(\chi^p) + q_{02}(\chi^n), \quad g_0(\chi) = g_{01}(\chi^p) + g_{02}(\chi^n)$$

where, the first (second) function in each equation represents the known parametric (nonparametric) component. The SDNNs for estimating the nuisance function q is represented in below:

$$\begin{aligned} Y_{it} &= q_{01}(\chi_{it}^p) + V_{it}^1 \Gamma^1 + \varepsilon_{it} \\ V_{it}^1 &= \sigma(\gamma^2 + V_{it}^2 \Gamma^2), V_{it}^2 = \sigma(\gamma^3 + V_{it}^3 \Gamma^3), \dots \quad \dots, V_{it}^L = \sigma(\gamma^L + \chi_{it}^n \Gamma^L) \end{aligned} \quad (2)$$

where, V^l are nodes at the l th layer, Γ^L are weights that map the data to the outcome via the intermediate nodes, and $\Gamma^{2:L}$ are weight matrices of dimensions equal to the number of nodes of the l th layer and the next layer up. The activation function $\sigma(\cdot)$ accommodates the nonlinear functional mappings by converting the input signal (from the previous layer) to an output signal of the current layer. Common choices are sigmoids, hyperbolic tangent, and ReLU. The number of layers and the number of nodes per layer are predetermined hyperparameters. A similar SDNN can be designed for estimating g , when replacing the outcome by T_{it} . Because the top layer is a linear model in χ^p and the derived variables V_{it}^1 , covariates in the parametric component χ^p have linear relationships with the treatment and outcome. We train the SDNNs by minimizing a loss function

which is defined as weighted sum-of-square errors between the true value and model estimates. See Web Appendix A for the underlying mathematics. A detailed instruction of how to enable SDNNs in ORF using Python is provided in Web Appendix B.

PRICE SENSITIVITY AND LIVE LIFE-CYCLE

Model Operationalization, Identification and Estimation

We now apply ORF to estimate how price elasticity varies over Live life-cycle. In this case, the target feature is the number of days to scheduled livestreaming day. We consider 29 test points within the window of 14 days before and after livestreaming day, i.e., $\{-14, -13, \dots, 0, \dots, 13, 14\}$. For each test point, ORF first assigns a set of similarity weights across observations using a forest-based kernel learner (as described in Algorithm 2 of Web Appendix A); and then estimate reduced form relations of log-transformed price and sales, conditional on all of the available covariates as shown in Table 1, by applying kernel SDNNs with the set of weights. This step is purely a prediction problem and the hyperparameters are suitably chosen to maximize out of sample fit.¹⁰

Among the available covariates summarized in Table 1, we pass 1,458 dummy indicators into the parametric component. They are creator fixed effects (to control for unobserved creator characteristics), Live topic category fixed effects, and various time fixed effects (including transaction/livestream week, transaction/livestream day-of-week, and temporal distance to livestream). Note that we do not include creator fixed effects in the price equation because 60% of creators only held one Live and there is limited within-Live price variation. For the remaining 242 covariates, we pass them into SDNNs to allow for all sorts of non-linearity and interactions. Details are provided in Web Appendix B and C.2.

Given the data generating process and our modeling approach, the identification of the price elasticity at each temporal distance to livestream is based on cross-sectional variation in Live prices

¹⁰We have also used kernel Lasso to estimate price and demand equations. We find that the out of sample fit is much lower than that of SDNNs (see Web Appendix C.1 for details) and the estimates of price elasticity are highly sensitive to hyperparameters. This suggests that the use of SDNNs is necessary for improving the explanatory power of covariates.

and demand. Specifically, the price elasticity at each test point (i.e., temporal distance to scheduled livestream day) is identified using estimated out-of-sample residuals via a kernel linear regression and by leveraging the cross-Live variation in these residuals. The key identification assumption is the unconfoundedness assumption, i.e., after conditioning on the rich information observed by the platform, the remaining variation in price is plausibly exogenous. In other words, the richness of covariates and flexible functional forms of the SDNNs allows us to project out the systematic component of creator pricing rule. This allows for the “discovery” of shocks that lead to exogenous price variation. While it is true that there is no way to empirically test this assumption, there are three reasons why we think that this assumption is likely to be satisfied in our study. First, our data are exceptionally detailed and rich (see Table 1), allowing us to control for all of the relevant observables. Second, the use of techniques such as SDNNs allows for all of the potential transforms and interactions among the observables. Finally, in subsequent sections, we show via multiple analyses that our results are robust to various sampling choices and model specifications.

Main Results

The estimation results based our proposed methodology are reported in Figure 5. The figure shows how the price elasticity of demand changes over Live life-cycle, along with the 95% confidence intervals obtained via 100 bootstrap samples.¹¹ Over the pre-livestream period, price elasticity is significantly negative, but becomes less negative over time. Price elasticity actually reaches zero on the livestreaming day. The post-livestream demand is still price elastic, but it is overall much less elastic than the pre-livestream demand. The difference between the pre-livestream and post-livestream price elasticity can be as large as 80%. Given that a significant proportion of sales happen on the livestreaming day, our research findings confirm that the live content format is highly valued by consumers in this market. In addition, our research findings suggest that the recorded version has substantial “residual value” as it accounts for about 22% of sales and its demand is actually less price elastic than the demand for the live version.

¹¹Figure 5 shows a small magnitude of fluctuation over the pre-livestream period. This may be driven by the fact that the number of unique Lives involve at each temporal distance are different over pre-stream period.

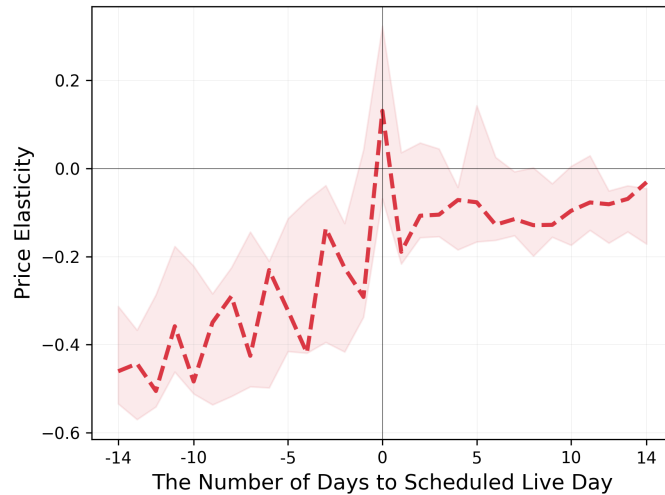


Figure 5: Price Elasticity over Live Life-Cycle

Note: The shaded region depicts 95% confidence interval via 100 bootstrap samples.

Note that the magnitude of price elasticity is small in most cases, between -1 and 0 , suggesting relatively inelastic demand for Lives. A natural question to ask is why creators do not raise prices. This is most likely due to the fact that there are known norms established for live events in a given market and event providers usually do not set prices outside these norms. This has been documented in previous research for many types of live events, such as concerts and performing arts (e.g., Felton 1992; Pompe, Tamburri, and Munn 2018). Even though Zhihu had a virtual monopoly on livestreaming over our study period, we thought it would be helpful to look at prices for comparable events on other livestreaming platforms during the same time period. As can be seen from Web Appendix D, Zhihu’s prices defined the upper bound of pricing for such events. This suggests that price norms did exist in this market and also that there was little room for creators on Zhihu Live to increase their prices.

Other Identification Concerns and Robustness Checks

In addition to the sources of endogeneity that we address in the main specification, there may exist other potential threats to our identification. We conduct several robustness checks to address these identification concerns.

Only the first Live per creator. Although about 60% of creators only hosted one Live in our data period, other creators may adjust pricing strategy over time as they gain more experience with the Live market in a way that is not fully controlled by our observables. If this is an important source of bias, we would expect our main results to be significantly different from the results based on each creator’s first Live, as this subset of Lives may free from such biases. Therefore, we repeat our main analysis by only using transactions associated with each creator’s first Live. The estimation results are shown in Figure W1 of Web Appendix E. We find that the estimated temporal patterns are robust to this subset of observations. Thus, we conclude that unobservables associated with state dependence in price setting and demand is not a concern in our study.

Controlling for creator-specific time trend. There may exist time-varying unobserved creator characteristics that are not fully captured by creator fixed effects in our main specification. These time-varying unobservables could lead to, for example, different trends in demand over temporal distance to livestreaming across creators. To alleviate this concern, we add interaction terms between creator indicators and temporal distance indicators in the parametric components of SDNNs in the demand equation, allowing differential time trends across creators. The estimation results are shown in Figure W2 of Web Appendix E. We find that our estimation results have little change, suggesting that time-variant unobservables are not a concern in our context.

Excluding extreme consumers or Lives. It is possible that a small group of heavy consumers is driving the main estimation results. We therefore order consumers according to their total number of purchases, and repeat our main analysis while removing the top 1% of consumers. The estimation results are shown in Figure W3 of Web Appendix E. We find that our main results are robust to the exclusion of these extreme consumers. In addition, it is possible that the estimated price elasticities are driven by extremely expensive Lives. To test this concern, we remove 12 Live events whose price is higher than 100 RMB. The estimation results are presented in Figure W4 of Web Appendix E. We find that removing these Lives makes little difference to our estimation results. In sum, our research findings are not driven by extreme buyers nor Lives.

Identification using instrumental variables. As mentioned previously, we are not able to empir-

ically test the unconfoundedness assumption. This is analogous to challenges inherent in validating the choice of instrumental variables for causal attribution. Nevertheless, as one additional method to test the key identification assumption of unconfoundedness, we use the approach described in Chernozhukov et al. (2018) that extends DML via the incorporation of instrumental variables, denoted as DMLIV. These instrumental variables, whose validity depends on institutional setting and data generating process, allow the researcher to control for the presence of unobserved confounders. We construct two instruments by utilizing the unique features of Lives. The first is the number of picture messages (e.g., prepared slides and photos) a creator sent in the Live chat room during the livestream. The second is the average thumbs-up on messages posted by the creator. The first variable is a measure of the effort put in by the creator into the Live (preparing for content is “costly”) while the second is reflective of the Live quality (as evidenced by the real-time audience). As a result, both these variables are likely to be correlated with the price of the Live, but uncorrelated with demand, as consumers do not have access to this information prior to purchase. We estimated the average pre-Live and post-Live price elasticities, respectively, using DMLIV and DML.¹² If the unconfoundedness assumption is violated, the results from the DMLIV and DML are likely to be different (regardless of the validity of the instruments). However, we find that both approaches give rise to similar results. Details are in Web Appendix F.

MECHANISMS

In this section, we explore the mechanisms that are driving our main results in Figure 5. We first show evidence for two main drivers of the observed pattern of results: (1) consumers value the opportunity of real-time interaction with content creators, and (2) consumers face different levels of quality concerns over the event life-cycle. Next, we investigate three alternative explanations, including consumer differences in observed characteristics or purchase preferences, the uncertainty in time availability for future consumption, and the option value of waiting. We find that none of

¹²This is because the DMLIV and DML are designed primarily for average treatment effect estimation and cannot flexibly capture heterogeneous treatment effect in a non-parametric manner.

these alternative explanations can fully explain the dynamics in price elasticity over Live life-cycle.

Real-Time Interaction Matters

We start by examining the inelastic demand on livestreaming day. The most intuitive explanation is that consumers place very high value on the opportunity of immediate real-time interaction with content creators. As noted earlier, on Zhihu consumers who purchase after seats are filled up can no longer interact with creators during livestream. This gives us a unique opportunity to examine how the availability of real-time interaction with content creators may influence price elasticity of demand. In this analysis, we focus on 317 Lives for which seats were filled up within one week prior to the livestreaming day.¹³ This means that consumers who buy a ticket on the livestreaming day for these Lives get the identical experience with one notable exception — they cannot interact with these creators. Thus, if the willingness-to-pay for these Lives on the day of the livestream is the same as the willingness-to-pay for Lives that have not sold out by the day of the livestream, then the conclusion is that the chance to interact does not change willingness-to-pay.

Accordingly, we estimate the price elasticity of demand on the day of livestream using data from these 317 Lives. We find that the price elasticity on the livestreaming day for these Lives is -0.283 (with a 95% confidence interval of [-0.128, -0.355]), in contrast to the approximately zero elasticity for all Lives reported in Figure 5. This suggests that the chance to interact with creators (i.e., the availability of the “interactive” tickets) is a driver of consumer willingness-to-pay.

To further test this, we examine how the price elasticity of daily demand changes relative to the day that seat limit was reached. Recall that the cumulative sales number is explicitly displayed on the page of each Live and the seat limit is 500 most of the time, so consumers may infer the number of remaining seats. We apply our model to these 317 Lives for which seats were filled up within one week prior to the livestreaming day. We set the number of days relative to the day that a Live’s seats are filled up as our target feature. The estimation results are displayed in Figure 6. As can be seen from the figure, there is an increasing trend before seats are filled up, and the

¹³The one week cutoff is conservative as a longer cutoff would make our result even stronger. We find that our results are robust if we use the data on all 583 Lives that were filled up before the streaming day.

elasticity reaches zero around two days before the filled-up day. But there is a sharp decreasing trend immediately after the filled-up day. These patterns suggest that as the seats are about to be filled up, demand becomes less price sensitive, even when livestream will occur a few days later after purchase. It is important to note that the number of remaining seats could be at play only when consumers value the opportunity of real-time interaction with content creators. Taken all together, these results confirm that the opportunity of real-time interaction with creators is an important consideration for consumers when purchasing Live events, regardless of whether these events are streamed on the day of purchase or a few days after purchase.

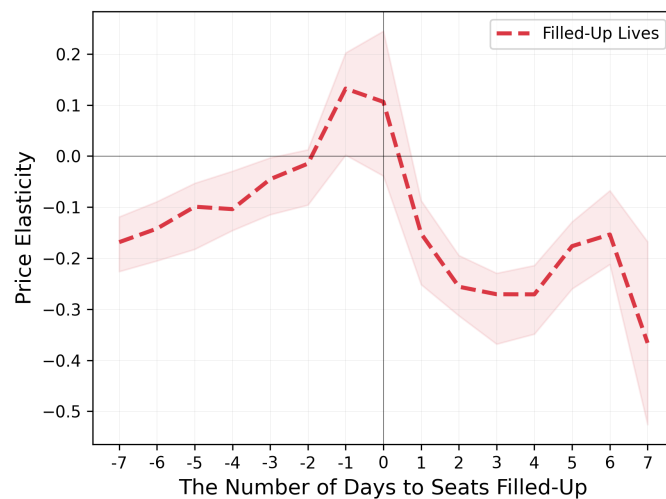


Figure 6: Price Elasticity Before and After Seats are Filled Up

Note: The shaded region depicts 95% confidence interval via 100 bootstrap samples.

Quality Matters

We now turn to the mechanism driving the less price-sensitive demand over the post-livestream period. As noted earlier, consumers on Zhihu face high quality uncertainty, due to the experiential nature of knowledge goods and the fact that most creators host only one Live on the platform. But the quality uncertainty is likely to be lower for the recorded version than the live version, given consumer ratings and reviews are only available after the Live has concluded. Thus, we examine whether quality matters for consumer willingness-to-pay. If this is true, demand should be less

price sensitive for Lives with higher quality (Okada 2010; Tsui 2012).

In our study context, the most important measure of Live-specific quality is ratings that are provided (on a 5-point scale) by consumers who have already purchased and consumed a Live. An average rating score, based on all of the individual ratings, is displayed on each Live’s webpage for consumers who may be interested in purchasing the recorded version. We find that about 95% of Lives have a rating between 3 and 5. We apply our model using rating score as the target feature and consider six test points evenly distributed over the interval [3,5]. As the rating of a Live is only available after its livestream ends, we examine the impact of rating score on price elasticity of post-livestream demand. The estimation results are shown in Figure 7. Consistent with our expectation, we find that demand is significantly less price sensitive when rating is higher. For example, price elasticity is on average 65% lower with a rating of 5 than with a rating of 3. In conclusion, our research findings suggest that consumers have much higher willingness-to-pay for higher quality, confirming the importance of content quality.

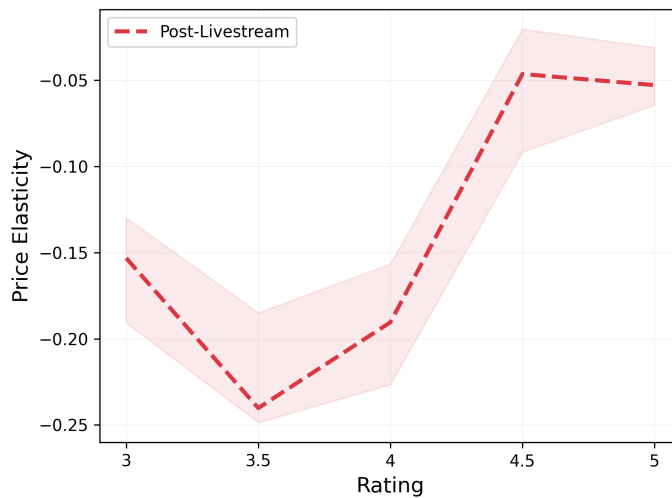


Figure 7: Price Elasticity and Consumer Rating Score

Note: The shaded region depicts 95% confidence interval via 100 bootstrap resamples.

Quality Uncertainty and Information Cues

We now look at other aspects of the institutional setting that could help strengthen our findings regarding the importance of Live quality. We rely on the idea that consumers are likely to leverage information cues to lower uncertainty at the time of purchase, especially when uncertainty is high (Urbany, Dickson, and Wilkie 1989). We focus on four sets of cues that consumers may leverage in our context: social proof, creator credibility, Live topic and consumer prior knowledge on creators. The key pattern we expect is that, given that there is a lot more information for the recorded version, consumer reliance on these cues will be higher in the pre-period relative to the post-period.

Social proof. One important way for consumers to infer quality is through popularity information (Cai, Chen, and Fang 2009; Tucker and Zhang 2011), e.g., the number of consumers who have already purchased a Live. We apply our model to pre- and post-livestream demand separately while setting the (log-transformed) cumulative demand of a Live as our target feature. Figure 8 reports the results. We find that over pre-livestream period, demand becomes much less price elastic as cumulative demand increases. In contrast, price elasticity of demand for recorded version is always inelastic to cumulative demand. These results provide evidence that consumers rely on social proof to make their purchase decisions only over pre-livestream period, i.e., when the quality uncertainty is high. One may argue that the cumulative demand just acts as a proxy for the temporal distance to livestreaming day. To tease out the effects of these two variables, we set the cumulative demand and the temporal distance as our target features simultaneously. The estimation results are shown in Figure 9. We find that the patterns in Figure 8 can be replicated at every temporal distance, confirming that the social proof mechanism is present over pre-livestream period regardless of the temporal distance. We want to note that the social proof mechanism not only explains the less price-sensitive demand over post-livestream period, but also sheds light on our main finding that pre-livestream demand becomes less price elastic toward the livestreaming day.

Creator credibility. Previous literature on reputation building suggests that consumers often rely on seller credibility to infer product quality, and tend to have higher willingness-to-pay if seller

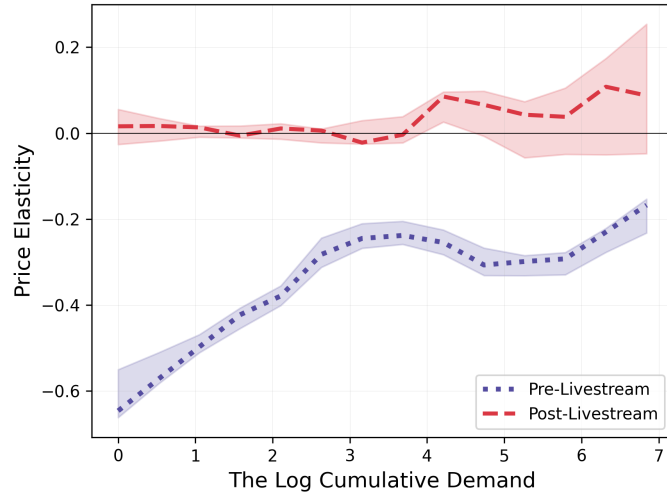


Figure 8: Price Elasticity and Cumulative Demand

Note: The shaded region depicts 95% confidence interval via 100 bootstrap samples.

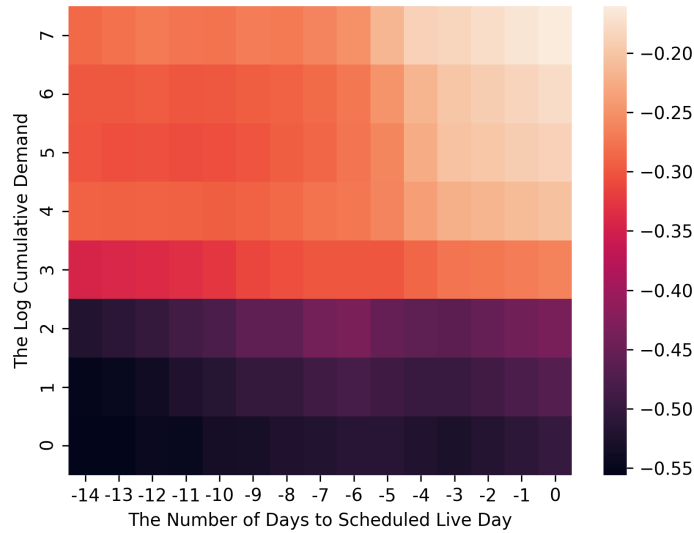


Figure 9: How Price Elasticity Varies over Live Life-Cycle and by Cumulative Demand

Note: We repeat ORF estimation using all the pre-livestream observations, while setting both cumulative demand and temporal distance as target feature. We consider a grid of $98 = 7 \times 14$ test pairs.

has higher credibility (Tellis 1988; Bolton 1989; Bijmolt, Van Heerde, and Pieters 2005; Hitsch, Hortacsu, and Lin 2019). On Zhihu, a creator’s total number of followers is the most important indicator of his/her expertise and reputation in the Q&A community (Toubia and Stephen 2013;

Goes, Lin, and Au Yeung 2014). Therefore, we expect that consumers are less price-sensitive to Lives hosted by creators with a larger number of followers, especially over pre-livestream period. To test this, we apply our model in each time period while setting a creator’s *follower share* as our target feature. The follower share indexes a creator’s number of followers relative to the largest number of followers among creators who host Lives in the same topic category.¹⁴ So a value of one indicates that a creator has the largest number of followers in a topic category. The estimation results with 10 evenly distributed test points are shown in Figure 10. One can see an increasing trend in both periods, confirming that demand is less price sensitive for creators with higher reputation. Interestingly, we find that as the follower share reaches one, demand becomes price inelastic or even exhibits slightly positive elasticity. In addition, the slope is significantly sharper over pre-livestream period than over post-livestream period. This is consistent with our previous argument that consumer reliance on information cues is higher in the pre-period relative to the post-period.

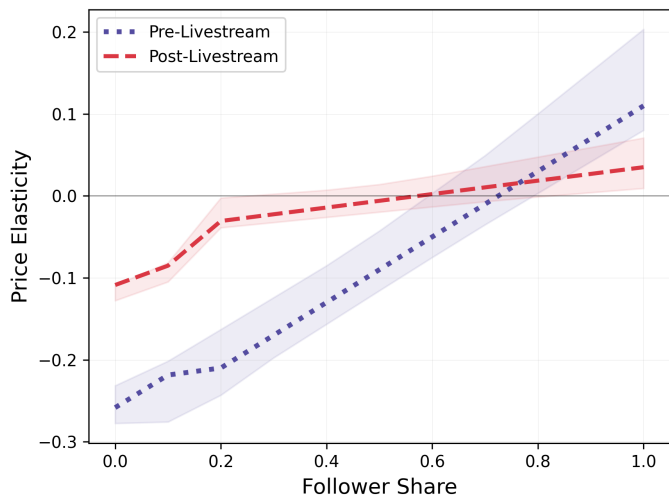


Figure 10: Price Elasticity and Creator Reputation in the Q&A Community

Note: The shaded region depicts 95% confidence interval via 100 bootstrap samples.

Live topic category. Consumers can also mitigate uncertainty about a purchase decision using

¹⁴We first compute the cumulative follower number of each creator i by the time of his/her Live j that belong to topic k , denoted as F_{ijk} . Because there is very large heterogeneity in interest across topics on Zhihu, the number of followers is more likely to be a fair indicator of creator credibility when comparing across creators who contribute the same topic category. Thus, for each topic k we obtain the maximum number of followers across all the creators who contributed topic k , denoted as M_k . Lastly, we define creator i 's follower share for topic k as $F_{ijk}/M_k \in [0, 1]$.

product category characteristics (Bettman 1974; Scattoni 1995). For example, a product might be perceived to be of lower quality when there is higher quality variance in the corresponding category. In particular, soft categories are shown to have higher perceived quality uncertainty than hard categories (Bebko 2000; Dai, Chan, and Mogilner 2020). Across all 17 topics available in Zhihu Live market, we label nine topics as *soft* topics (Internet, Psychology, Education, Travel, Life Style, Food & Cuisine, Career, Reading & Writing, Music/Game/Movie), while the other eight topics that are relatively objective as *hard* topics (Law, Business, Econ & Fin, Healthcare, Architecture & Interior Design, Art Appreciation & History, Science & Technology, Sports) based on our common knowledge. We indeed find that the variance of consumer ratings across Lives for soft topics is significantly higher than that for hard topics ($p < 0.05$). We apply our model to understand how price elasticity of demand varies across topic categories over each time period. The results are shown in Figure 11. We find that on average demand is much more price sensitive for soft topics (the nine topics on the right) than for hard topics (the eight topics on the left), over both time periods. This confirms our assertion that quality uncertainty level differs across topics and hence affects consumer purchase decision. In addition, we find that the differences of price elasticities between the soft and hard topics tend to be higher over pre-livestream period than over post-livestream period. This suggests that consumers are more likely to rely on topic to make a purchase decision of live versions than of recorded versions, further confirming our proposed quality uncertainty reduction mechanism.

Consumer prior knowledge. Consumers can also infer the quality of a Live from their own prior knowledge about its creator. One important way to acquire this knowledge is through following creators' content contribution activities in the free Q&A community. As such, we split all of the transactions into two groups based on whether each consumer had followed the creator before making a purchase. We find that about 20% of consumers have done so, and these consumers generated about 17% of transactions in our data. We label this group of consumers as "high prior knowledge" group, while label others as "low prior knowledge" group. For each group, we aggregate all of the transactions at Live-day level, and repeat our main analysis. Figure 12 shows the results. First, the

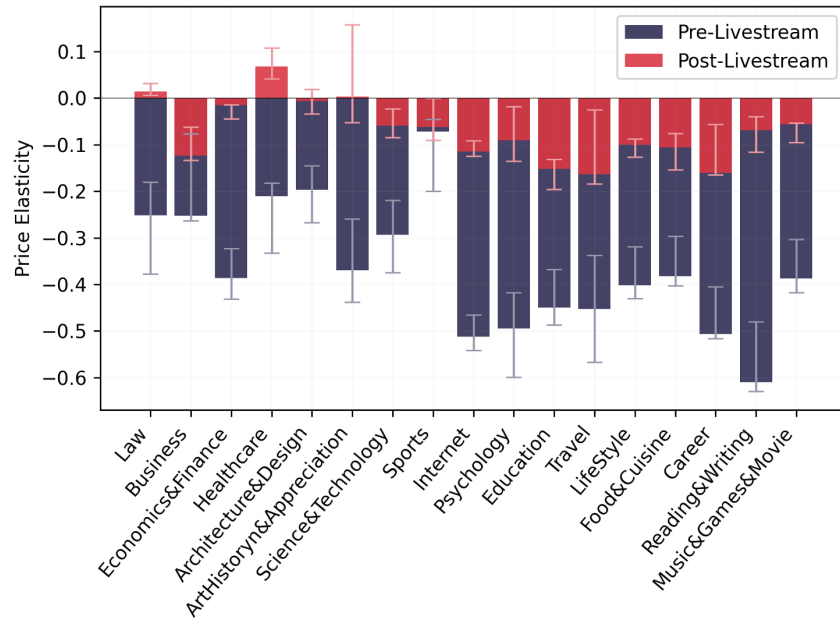


Figure 11: Price Elasticity and Live Topic Category

temporal dynamics shown in Figure 5 are replicated in both consumer groups. Second, the group with high prior knowledge is significantly less price sensitive than the low group at all temporal distances, except for a few days around livestreaming day. This observation confirms that prior knowledge can influence consumer perceived quality and hence price elasticity. Third, the differences in price elasticities between these two consumer groups become smaller over Live life-cycle. This pattern implies that consumers are much less likely to rely on their prior knowledge to resolve quality uncertainty of recorded versions than of live versions.

In conclusion, we find that consumers value recorded content and this can be explained by lower quality uncertainty of finished Lives. This finding complements previous findings for live events whose consumption is driven by event outcomes, e.g., sporting events. For such events, consumers prefer watching them live even though tape-delayed broadcasts provide the same content (Vosgerau, Wertenbroch, and Carmon 2006). In contrast, creator-generated livestreaming content, such as Live events studied in this paper, is not focused on outcomes and results, making the recorded content relevant and valuable.

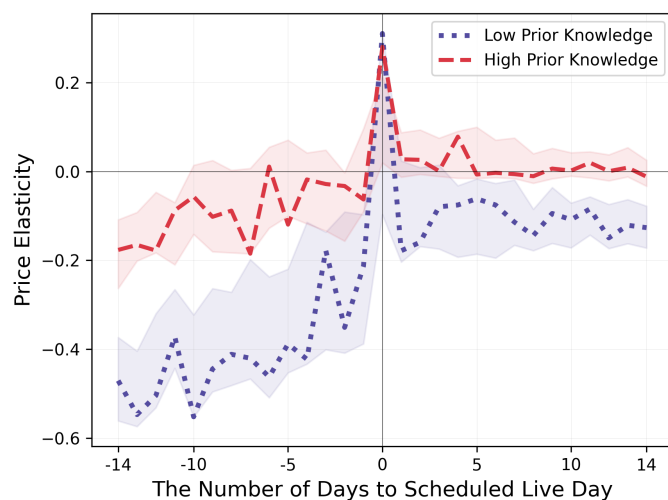


Figure 12: Price Elasticity and Consumer Prior Knowledge

Note: The shaded region depicts 95% confidence interval via 100 bootstrap samples.

Other Possible Explanations

We conclude this section by ruling out three alternative explanations that may drive the temporal dynamics in price elasticity of demand.

Consumer differences in observed characteristics. One possibility is that different types of consumers arriving to purchase at different time. To investigate this, we first examine differences in observables by zooming in on three major types of consumer characteristics on the platform that are highly associated with consumers' levels of experience, engagement, and reputation: consumer lifetime, followee size, and follower size in the Q&A community.¹⁵ We regress each dependent variable at the time of purchase on the fixed effects of temporal distances to livestreaming day, while controlling for transaction calendar-day fixed effects and Live characteristics shown in Table 1. We focus on transactions from 14-day before to 14-day after livestreaming day, resulting in over 1.2 million observations for each regression model. The estimated fixed effects of temporal distances are displayed in Figure W5 of Web Appendix E. We find that the estimates are quite noisy and their differences are mostly insignificant (or very small in magnitude if significant). Therefore,

¹⁵We use consumer characteristics in the Q&A platform rather than those in the Live market because about 80% consumers only purchased one Live in our data.

it seems unlikely that differences across these observables could account for the big change (about 80%) in consumer price elasticity from the pre-period to the post-period. Therefore, we conclude that differences in observed consumer characteristics are unlikely to be the main driver of the dynamics in price plasticity over Live life-cycle.

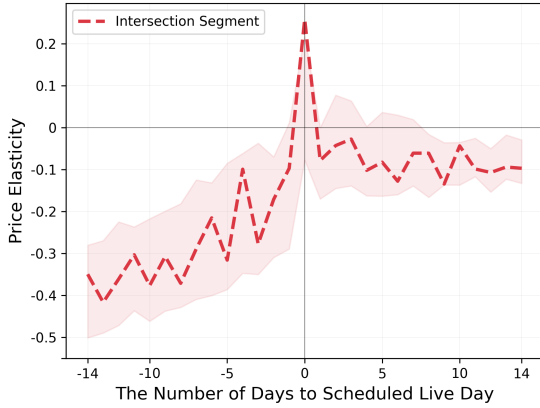
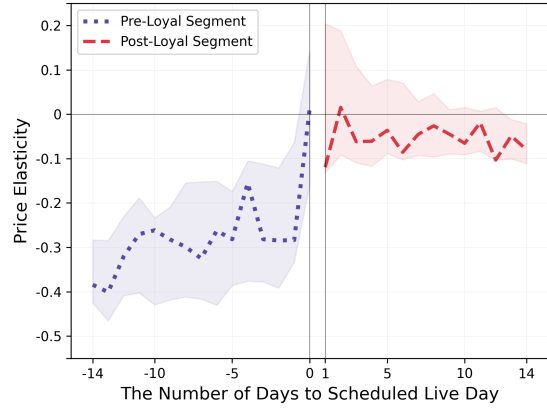
Consumer differences in purchase preferences. Consumers may vary systematically on their preferences for consuming live versus recorded content. For example, consumers who purchase before or on the livestreaming day are likely to be those who value live interaction and would like to pay more for livestream. Likewise, consumers who always purchase the recorded versions may be willing to pay as much or more for the recorded version than the live version. To investigate this, we partition all the consumers into three segments: pre-loyal (consumers who have only purchased before day of livestream), post-loyal (consumers who have only purchased access to recorded versions of Lives), and intersection (consumers who have purchased Lives in both periods). Table 6 compares the three consumer segments along a few dimensions. We find that the intersection segment, comprising 20% of all consumers is the most active of the three on the platform, generating 64% of the transactions. For each consumer segment, we recompute daily demand, and then apply ORF to repeat our main analysis, but the difference is that the price elasticity of pre-loyal (post-loyal) segment can only be estimated for $d \in [-14, 0]$ ($d \in (0, 14]$). The estimation results are shown in Figure 13. We find that the temporal dynamics shown in Figure 5 can be replicated across all of the three consumer segments. In addition, we find similar magnitudes of the estimated price elasticities across different scenarios. In conclusion, there seems to be no evidence that the temporal dynamics in price elasticity are driven by consumer self-selection based on preference for live versus recorded version.

Uncertainty in the time availability for future consumption. Consumers may be uncertain about their availability to participate in a Live event that will be streamed in a few days later after purchase. This may lead to a declining magnitude in price elasticity closer to the live day and a less elastic demand in the post-period as consumer uncertainty about availability is resolved. If this is the mechanism at play, we would expect the demand to be less elastic for consumers who have

Table 6: The Three Consumer Segments

	Intersection	Pre-loyal	Post-loyal
Num. Consumers	181,233	537,938	183,766
% Consumers	20	59	21
% Transactions	64	26	10
Num. pre-purchases	7.66 (272.96)	1.80 (21.20)	0.00 (0.00)
Num. post-purchases	2.99 (11.95)	0.00 (0.00)	1.27 (2.24)

Note: The last two rows report the average (pre-stream and post-stream) purchases per consumer within each consumer segment, with the standard deviation in parentheses.

**(a)** Price Elasticity of the Intersection Segment**(b)** Price Elasticity of the Pre-loyal and Post-loyal Segment**Figure 13:** Price Elasticity over Live Life-Cycle across Consumer Segments

more free time and hence are less uncertain about their future availability. To investigate this, we compute the proportion of voting activities that each consumer i has engaged across each day of week over one-year before and after the launch of Zhihu Live program, denoted by $Share_{iu}$ for $u \in \{1, 2, \dots, 7\}$.¹⁶ A consumer is considered to have more free time at a given day of week u , if he has a higher value of $Share_{iu}$. For each Live j streamed on day of week u , we divide consumers into low and high (availability) uncertainty groups based on whether their values of $Share_{iu}$ ex-

¹⁶We focus on user voting activity because it occurs more frequently than other user activities such as content contribution. There are 340,037 consumers who do not have voting activities over the two-year window. We excluded them from our analysis.

ceed the medium level across all of the consumers of that Live. For each group, we aggregate all of the transactions at Live-day level, and repeat our main analysis. Figure W6 of Web Appendix E presents the results. We find that the trajectories of the low-availability and high-availability groups do not significantly differ from each other, suggesting no evidence that consumer availability at livestreaming day drives our main results.

The option value of waiting. If a consumer purchases a Live early, the consumer will forego the utility that could be derived from other options with the money. As the day of the livestream gets closer, such opportunity cost may decline, so consumer willingness-to-pay may increase. If this is the dominant driver for the pattern in our main results, consumer willingness-to-pay on livestreaming day should always be high, regardless of whether seats are available. However, as shown in the subsection *Real-Time Interaction Matters*, we find a significant negative price elasticity on the live day for Lives whose seats were filled up prior to livestream. In addition, during our study period, there were very few new Lives created in each week (an average of 10 Lives) for consumers to choose from. This suggests relatively low value of waiting, especially when consumers have preferences for specific topics. In sum, we conclude that the declining option value of waiting is unlikely to be the major driver of our main results.

MANAGERIAL IMPLICATIONS

Our research findings have important managerial implications for platforms and creators. First, our results confirm that what makes livestreaming an engaging medium is the opportunity of real-time consumer-creator interaction. Second, and more surprisingly, our results show that live content has value beyond the live part. In other words, there is considerable value in the content that is not centered in its live attribute. For creators, this means that they should seek out platforms that allow monetization of livestreaming *and* recorded content. In addition, they could explore ways to adapt their livestream style and content such that it results in more engaging recorded versions. For platforms, they need to think more carefully about whether and how to offer both types of content consumption — live and recorded — for their viewers. Offering both can enhance revenues for

both creators and the platform.

In addition, our research findings suggest that reducing (quality) uncertainty about upcoming events are important considerations for all parties (consumers, creators, and platforms). Specifically, platforms can improve their online rating system and other operating policies (e.g., filtering and search functions) to reduce information asymmetry. Creators can benefit from providing detailed descriptions of upcoming events and building reputation in general. Further more, our research findings suggest opportunity for platforms and creators to implement dynamic pricing, promotion, and targeting. For example, it could be beneficial for platforms and creators to target consumers who have lower uncertainty (e.g., followers of creators) in the days after the livestream is announced and available for sale. In contrast, consumers who are very quality sensitive could be good targets for the recorded versions of Lives. Also, from the platform's perspective, it appears that price promotions are going to be more effective early in the pre-livestream as demand is (relatively) more sensitive to price then.

Besides these aggregate, platform-level implications, our results can also be used at the level of individual Lives, especially in terms of deciding prices for the pre- and post-livestream periods. We carry out a policy simulation to estimate the optimal prices for a given creator's Live offering (details on the simulation are provided in Appendix B). Specifically, we can compute the optimal prices for a Live as a whole or as a two-part pricing, i.e., a different price for pre-livestream and post-livestream (given the simplifying assumptions that consumers are myopic and demand has no state dependence). The policy simulation provides three sets of interesting and potentially useful findings. First, on average, Lives are under-priced by about 60% on Zhihu. Thus, creators should explore raising prices, while keeping the general norms (discussed earlier) in mind. Second, it turns out that creators who have a stronger (weaker) reputation tend to over(under)-price their events. Thus, creators should adjust their prices upward or downward based on their reputation. Finally, we find that a two-part pricing is likely to be revenue enhancing for creators, and this is especially true for less-established creators who may have a stronger willingness to boost sales.

CONCLUSIONS, LIMITATIONS AND FUTURE RESEARCH

This paper represents one of the very early studies on the fast growing phenomenon of livestreaming. While there is a widespread belief that the value of livestreaming lies in its live part, there is virtually no research that has examined this. This paper contributes to this research domain by leveraging rich data from a large livestreaming platform. Taking advantage of the fact that the platform also provides access to recorded, non-live, content at the same price as for the live content, we document the time-varying price responsiveness of demand over the entire event life-cycle. We do this via the use of state-of-the-art methods in machine learning that allow us to carry out causal inference in new and complex settings such as livestreaming with observational data. We find that demand becomes less price-sensitive gradually over time to the scheduled live day and is inelastic on the day of livestream. Over the post-livestream period, demand for the recorded version is still price elastic, but surprisingly, it is much less sensitive than the pre-livestream demand.

We further provide consistent evidence for two important factors that drive our main results. First, we show that consumers highly value the opportunity of real-time interaction with creators. This lowers their price sensitivity dramatically, leading to demand getting more and more inelastic as the day of the livestream gets closer. Second, we show that the reduced price sensitivity of demand for recorded version can mostly be attributed to quality uncertainty reduction. It turns out that consumers are much better at assessing content quality after the event concludes, leading to a lower price sensitivity for the recorded version on average.

Methodologically, we demonstrate a novel approach for heterogeneous treatment effect estimation using observational data under high-dimensional confounders. In particular, we generalize ORF via the use of SDNNs for nuisance estimation. This adaptation is well suited to panel data because it can handle clustering effect via fixed effects, while allowing for nonlinear transformation of other covariates. We believe that this framework will be useful for heterogeneous treatment effect estimation in many real-world settings, where active experimentation may be difficult and there can be a large amount observational data for which the treatment policy is unknown, such as

peer-to-peer markets or gig-economy platforms.

We hope this paper will stimulate further empirical study of livestreaming markets, as our study has some limitations, mostly driven by the data. First, we use data from a single livestreaming platform where creators provide paid live events. Second, we do not have granular data in terms of how consumers engage with such content (e.g., minutes watched, comments, Q&As, pausing and repeat watching of recorded content). Access to such data can help understand the drivers of consumer consumption in more detail. Third, as noted earlier, the creators in our sample are compensated via direct pricing. Livestreamers who are compensated by indirect pricing (e.g., via brand sponsorships) may deliver content and engage with consumers during live events in different ways. Future research could explore these possible research directions.

REFERENCES

- Athey, Susan, Julie Tibshirani, and Stefan Wager (2019), “Generalized random forests,” *The Annals of Statistics*, 47 (2), 1148–1178.
- Athey, Susan and Stefan Wager (2019), “Estimating Treatment Effects with Causal Forests: An Application,” *arXiv preprint arXiv:1902.07409*.
- Bebko, Charlene Pleger (2000), “Service intangibility and its impact on consumer expectations of service quality,” *Journal of services marketing*.
- Bettman, James R (1974), “Relationship of information-processing attitude structures to private brand purchasing behavior.,” *Journal of Applied psychology*, 59 (1), 79.
- Bijmolt, Tammo HA, Harald J Van Heerde, and Rik GM Pieters (2005), “New empirical generalizations on the determinants of price elasticity,” *Journal of marketing research*, 42 (2), 141–156.
- Bolton, Ruth N (1989), “The relationship between market characteristics and promotional price elasticities,” *Marketing Science*, 8 (2), 153–169.
- Bound, John, David A Jaeger, and Regina M Baker (1995), “Problems with instrumental variables estimation when the correlation between the instruments and the endogenous explanatory variable is weak,” *Journal of the American statistical association*, 90 (430), 443–450.
- Cai, Hongbin, Yuyu Chen, and Hanming Fang (2009), “Observational learning: Evidence from a randomized natural field experiment,” *American Economic Review*, 99 (3), 864–82.
- Chernozhukov, Victor, Denis Chetverikov, Mert Demirer, Esther Duflo, Christian Hansen, and Whitney Newey (2017a), “Double/debiased/neyman machine learning of treatment effects,” *American Economic Review*, 107 (5), 261–65.
- Chernozhukov, Victor, Denis Chetverikov, Mert Demirer, Esther Duflo, Christian Hansen, Whitney Newey, and James Robins (2018), “Double/debiased machine learning for treatment and structural parameters: Double/debiased machine learning,” *The Econometrics Journal*, 21 (1).
- Chernozhukov, Victor, Matt Goldman, Vira Semenova, and Matt Taddy (2017b), “Orthogonal ma-

- chine learning for demand estimation: High dimensional causal inference in dynamic panels,” *arXiv preprint arXiv:1712.09988*.
- Chernozhukov, Victor, Matt Goldman, Vira Semenova, and Matt Taddy (2020), “Orthogonal machine learning for demand estimation: High dimensional causal inference in dynamic panels,” *arXiv*, pages arXiv–1712.
- CIW Team “Profile of Zhihu: China’s Quora, a top content community,” <https://www.chinainternetwatch.com/31732/zhihu-profile/> (2021) Accessed on June 7, 2021.
- Crane-Droesch, Andrew (2017), “Semiparametric panel data models using neural networks,” *arXiv preprint arXiv:1702.06512*.
- Dai, Hengchen, Cindy Chan, and Cassie Mogilner (2020), “People rely less on consumer reviews for experiential than material purchases,” *Journal of Consumer Research*, 46 (6), 1052–1075.
- Davis, Jonathan and Sara B Heller (2017), “Using causal forests to predict treatment heterogeneity: An application to summer jobs,” *American Economic Review*, 107 (5), 546–50.
- Felton, Marianne Victorious (1992), “On the assumed inelasticity of demand for the performing arts,” *Journal of Cultural Economics*, 16 (1), 1–12.
- Fergus “The Growth of Paid Knowledge Industry in China 2020,” <https://www.iimedia.cn/c1020/70056.html> (2020) Accessed on June 7, 2020.
- Goes, Paulo B, Mingfeng Lin, and Ching-man Au Yeung (2014), ““Popularity effect” in user-generated content: Evidence from online product reviews,” *Information Systems Research*, 25 (2), 222–238.
- Hitsch, Günter J, Ali Hortacsu, and Xiliang Lin “Prices and promotions in us retail markets: Evidence from big data,” Technical report, National Bureau of Economic Research (2019).
- Hu, Mu, Mingli Zhang, and Yu Wang (2017), “Why do audiences choose to keep watching on live video streaming platforms? An explanation of dual identification framework,” *Computers in Human Behavior*, 75, 594–606.
- Imbens, Guido W (2014), “Instrumental variables: an econometrician’s perspective,” *Statistical science*, 29 (3), 323–358.

- Iqbal, Mansoor “Twitch Revenue and Usage Statistics,” <https://www.businessofapps.com/data/twitch-statistics/#:~:text=Trafficcontinuedtogrow,with,1.4millioninQ12020.> (2021) Accessed on May 19, 2021.
- Larson, Kristin “Retailers Embrace Livestreaming, Market Expected To Reach \$11 Billion In 2021,” <https://www.forbes.com/sites/kristinlarson/2021/03/27/retailers-embrace-livestreaming-market-expected-to-reach-11-billion-in-2021/?sh=7ad6fae52fde> (2021) Accessed on May 19, 2021.
- Lin, Yan, Dai Yao, and Xingyu Chen (2021), “EXPRESS: Happiness Begets Money: Emotion and Engagement in Live Streaming,” *Journal of Marketing Research*, page 00222437211002477.
- Lu, Shijie, Dai Yao, Xingyu Chen, and Rajdeep Grewal (2021), “Do Larger Audiences Generate Greater Revenues under Pay What You Want? Evidence from a Live Streaming Platform,” *Marketing Science (forthcoming)*.
- Okada, Erica Mina (2010), “Uncertainty, risk aversion, and WTA vs. WTP,” *Marketing Science*, 29 (1), 75–84.
- Oprescu, Miruna, Vasilis Syrgkanis, and Zhiwei Steven Wu (2018), “Orthogonal Random Forest for Causal Inference,” *arXiv preprint arXiv:1806.03467*.
- Pompe, Jeffrey, Lawrence Tamburri, and Johnathan Munn (2018), “Subscription ticket sales for symphony orchestras: Are flexible subscription tickets sustainable?,” *Managerial and Decision Economics*, 39 (1), 71–78.
- Sands, Emily Glassberg “Machine Learning Meets Instrumental Variables,” <https://medium.com/teconomics-blog/machine-learning-meets-instrumental-variables-c8eecf5cec95> (2018).
- Scattone, Joan “Factors Influencing Consumer Perceptions, Attitudes, and Consideration of Sbs,” “AMA Summer Marketing Educators’ Conference Proceedings,” Chicago: American Marketing Association (1995).
- Statista (2020), “Market size of online live streaming in China in 2018 and 2019 with a forecast

- for 2020,” Available online at <https://www.statista.com/statistics/874591/china-online-live-streaming-market-size/#statisticContainer>.
- Tellis, Gerard J (1988), “The price elasticity of selective demand: A meta-analysis of econometric models of sales,” *Journal of marketing research*, 25 (4), 331–341.
- Thomas, Laurant and Annie Palmer “U.S. retailers scramble to crack the code on livestream shopping events,” <https://www.cnbc.com/2021/05/03/retailers-from-bloomington-to-petco-test-livestreaming-to-win-sales.html> (2021) Accessed on May 19, 2021.
- Toubia, Olivier and Andrew T Stephen (2013), “Intrinsic vs. image-related utility in social media: Why do people contribute content to twitter?,” *Marketing Science*, 32 (3), 368–392.
- Tsui, Hsiao-Chien (2012), “Advertising, quality, and willingness-to-pay: Experimental examination of signaling theory,” *Journal of Economic Psychology*, 33 (6), 1193–1203.
- Tucker, Catherine and Juanjuan Zhang (2011), “How does popularity information affect choices? A field experiment,” *Management Science*, 57 (5), 828–842.
- Urbany, Joel E, Peter R Dickson, and William L Wilkie (1989), “Buyer uncertainty and information search,” *Journal of consumer research*, 16 (2), 208–215.
- Vosgerau, Joachim, Klaus Wertenbroch, and Ziv Carmon (2006), “Indeterminacy and live television,” *Journal of Consumer Research*, 32 (4), 487–495.
- Wager, Stefan and Susan Athey (2018), “Estimation and inference of heterogeneous treatment effects using random forests,” *Journal of the American Statistical Association*, 113 (523), 1228–1242.
- Wheless, Erika (2021), “LG kicks off series of live stream shopping events produced in-house,” Available online at <http://ec2-34-225-151-148.compute-1.amazonaws.com/retail/lg-kicks-off-series-of-live-stream-shopping-events-produced-in-house/>.

APPENDIX

A. ZHIHU INTERFACE

The screenshot shows a Zhihu question page. At the top, there are topic tags: "NBA", "NBA 球员", "斯蒂芬·库里 (Stephen Curry)", and "巨星". The question title is "如果把库里放到上个世纪 90 年代, 还能否有巨星的表现?". Below the question, there are three answers, each enclosed in a red box. Answer 1 is by 张佳玮, Answer 2 is by 演无三点, and Answer 3 is by Air真心为你. Each answer includes the user's profile picture, name, and a brief bio. The answers discuss the impact of coaching and team dynamics on Curry's performance in the 1990s.

Topic tags
NBA NBA 球员 斯蒂芬·库里 (Stephen Curry) 巨星

Question title
如果把库里放到上个世纪 90 年代, 还能否有巨星的表现?

Answer 1
张佳玮
2021 新知答主
765 人赞同了该回答
巨星在哪个时代都会是巨星, 只看不同教练治下, 能巨成什么样了。
像马克·杰克逊带库里三年, 库里也就是全明星、联盟二阵。科尔一用库里, 库里立刻带队进王朝。
也不奇怪。达拉斯版本的纳什就是全明星, 太阳版本的纳什就是 MVP。太阳版本的基德就是个杰出后卫, 网版本的基德就是准 MVP。
看阵容, 看教练。
怎么用很重要。
展开阅读全文

Answer 2
演无三点
12 人赞同了该回答
能。
上世纪 90 年代, 非法防守还没被取消, 只要球队不是傻缺, 库里大概率能得到大量的一对一机会。而且就凭不能包夹弱侧无球人这一点, 以库里的无球跑位穿插能力, 对手得头疼死
至于handcheck, 对喜欢原地持球三威胁的人有用, 对库里真没多大用
发布于 2021-04-29 12:41

Answer 3
Air真心为你
动漫爱好者
235 人赞同了该回答
曾经有位知名答主 @静易 写过一个这样的回答如果巅峰期奥尼尔来现在的 NBA 打球会怎样? 里面的论点本人非常赞同
他的论断是: 即便奥尼尔放到现在的联盟, 同样具有高度的战略价值
所以基于同样的理由, 你问库里放到别的年代会怎样, 我同样会说, 库里放到别的年代, 同样具有高度的战略价值!
首先, 库里和奥尼尔, 代表着篮球这项运动的两个极端, 而且都是各自领域的佼佼者, 甚至库里更 bug。毕竟强如奥尼尔, 你也依然能从漫漫历史长河中找到许多和他同级别的人, 张伯伦, 拉塞尔, 贾巴尔, 大梦, 罗宾逊, 尤因, 他们虽然风格不尽相同, 但都是具备超强统治力的内线人物。但是, 库里在历史长河中, 你找不到一个模板, 没错, 一个也没有。即便诸如雷阿伦, 米勒这两位顶级射手, 他们会的库里也会, 甚至比他们更会, 库里会的, 他们却未必会。
所以, 库里和奥尼尔, 代表着篮球这项运动的两个极端, 就像答主 @静易 说的一样: 奥尼尔是历
展开阅读全文

Figure A1: Example of a Question and Its Answers



Figure A2: Example of User Profile Page

B. POLICY SIMULATION

In this section, we describe how to derive the optimal price of each Live, using the estimated price and demand functions in Equation (1). The predicted total revenue of a Live event j at price T over temporal distance interval $[D, \bar{D}]$ can be expressed as (for simplicity, we omit subscript j),

$$\Pi(T) = \sum_{d=D}^{\bar{D}} \left[(\hat{q}(X, W) - \hat{\beta}_d \hat{f}(X, W))T + \hat{\beta}_d T^2 \right],$$

Title: Things to consider when choosing a restaurant



Figure A3: Example of a Live Session

Note: This figure illustrates the interface of a Live. During the livestream, the creator will give a real-time talk via voice/text/picture messages. The creator can also address questions raised by consumers. Notice that only consumers who purchased the Live before seats are filled up are able to raise questions and leave comments during the livestream.

where X denotes the target feature, i.e., the temporal distance to the live day. $T, W, q(\cdot), f(\cdot)$ have the same definition as before. The variable $\hat{\beta}_d$ is the estimated price elasticity at a given temporal distance d . Note that throughout this policy simulation, we assume no state dependence of demand. Thus, we exclude the cumulative sales of a Live from covariate matrix W . By maximizing Live revenue Π , we can derive the optimal price T^* for Live j over temporal distance interval $[D, \bar{D}]$,

$$T^* = \frac{\sum_{d=D}^{\bar{D}} [\hat{q}(X, W) - \hat{\beta}_d \hat{f}(X, W)]}{\sum_{d=D}^{\bar{D}} \hat{\beta}_d}.$$

In particular, for each Live, we solve optimal prices for three temporal distance intervals $[-14, 14]$, $[-14, 0]$, and $(0, 14]$, denoted as T_{whole}^* , T_{pre}^* , and T_{post}^* .

Having obtained the optimal prices, we examine creators' pricing efficiency by comparing the

optimal price T_{whole}^* and the actual price observed in the data. We find that the average optimal price across Lives is 35.99 RMB, which is 61% higher than the average actual price in our data ($p < 0.000$). This suggests that under-pricing seems to be prevalent on this market. Meanwhile, the patterns varies largely depends on creators and Lives. In particular, we find that among creators who have a higher reputation and Lives that have a higher rating score, over-pricing seems to be more common ($p < 0.01$).

In addition, we examine the room for dynamic pricing over the pre- and post-period by comparing T_{post}^* and T_{pre}^* . We find that, on average, T_{pre}^* is 14.9% lower than T_{post}^* ($p < 0.01$). This suggests that setting a higher price over post-livestream period is an optimal choice for creators. This is intuitive given the less-sensitive demand over the post-livestream period. We further investigate the divergence between T_{post}^* and T_{pre}^* by defining $\Delta T^* = T_{post}^* - T_{pre}^*$. A larger positive value of ΔT^* implies a more aggressive and strategic dynamic pricing policy. To examine how ΔT^* varies across creators and Lives, we regress ΔT^* against a set of creator and Live characteristics that were used for the cross-sectional demand regression in the *Descriptive Analysis* section. We find that a Live's rating score has a positive and significant impact on ΔT^* , implying that creators can enlarge the price differences over the two periods if Live quality is expected to be high. Interestingly, ΔT^* tends to be smaller among creators who have more established reputation. This suggest that dynamic pricing may be more (less) necessary for less (more) established creators. The intuition for this finding is that the marginal benefits of dynamic pricing are high for less established creators who need to boost sales, while established creators who already have high demand volumns over both periods do not have to game.

WEB APPENDIX

A. DETAILS OF ORF ALGORITHM

Throughout this appendix, we simplify the problem set-up described in the paper by changing subscript of all variables/data from it to i . Algorithms 1 and 2 describe how to train the forest-based kernel learner. Algorithm 3 describes how ORF uses the forest-based kernel learner to perform kernel estimation.

Random Forest as a Weights Learner

We first describe the forest-based kernel learner, whose pseudo code is provided in Algorithm 2. This procedure relies on a few forest regularity conditions required for convergence. Please refer to [Opreescu, Syrgkanis, and Wu \(2018\)](#) for details. The random forest algorithm proceeds over B iterations. For each iteration b , it first randomly subsamples a subset S_b without replacement from the full dataset, which contains N observations $D = \{Z_i = (T_i, Y_i, W_i, X_i)\}$. The tree learner \mathcal{L}_T then randomly partitions S_b into two subsets of equal sizes S_b^1, S_b^2 . The learner uses S_b^1 to grow the tree (i.e., place splits in the tree), and uses the feature X_i in S_b^2 for stopping rules and balance maintenance. To ensure honesty of the tree ([Athey, Tibshirani, and Wager 2019](#)), \mathcal{L}_T does not select the splits using the controls and outcomes in S_b^2 , which will be used for kernel estimation later. That is, in order to reduce prediction bias, forests use only the first half of the randomly split subsample for splitting, while the second half for populating the tree’s leaf nodes: each new example is “pushed down” the tree and added to the leaf in which it falls. This is a key difference from classic random forests in which a single subsample is used both to choose a tree’s splits and for the leaf node examples used in predictions.

Similar to GRF, the tree learner starts with a root node that contains the entire feature vector space, iteratively grows the tree by greedily selecting the splits that maximize certain splitting criterion, until certain stopping condition is met. However, the key modification to GRF’s tree learner is the incorporation of orthogonal nuisance estimation (i.e., DML) in tree splitting criterion.

At each internal node P , \mathcal{L}_T will perform the following two-stage estimation for $\hat{\theta}_P$ over the set of observations in S_b^1 that reach P (denoted as $P \cap S_b^1$). First, the algorithm estimates the nuisance functions q_0 and g_0 , using any machine learning methods, such as lasso, random forest, and DNNs. Second, the algorithm uses the estimated nuisance functions, denoted as \hat{q}_P and \hat{g}_P , to residualize the outcome and treatment for each observation that reaches P :

$$\tilde{Y}_i = Y_i - \hat{q}_P(X_i, W_i), \tilde{T}_i = T_i - \hat{g}_P(X_i, W_i) \quad (3)$$

The residualization step partials out the confounding effects from X_i and W_i in each observation, so these residuals represent exogenous variation that can be used to identify a valid causal effect in a second stage regression (Chernozhukov et al. 2017a). Then, the second-stage estimation is obtained by regressing the residualized \tilde{Y} on the residualized \tilde{X} :

$$\hat{\theta}_P = \arg \min_{\theta} \frac{1}{|P \cap S_b^1|} \sum_{Z_i \in P \cap S_b^1} \frac{1}{2} (\theta \tilde{T}_i - \tilde{Y}_i)^2 \quad (4)$$

Given the estimate $\hat{\theta}_P$ at parent node P , we would like to split the parent node into two children C_1 and C_2 . Similar to GRF, we seek the split that maximize heterogeneity in the treatment effect estimates across children nodes. Namely, if we perform the same two-stage estimation separately at each child, the new estimates $\hat{\theta}_{C_1}$ and $\hat{\theta}_{C_2}$ will maximize the following heterogeneity score:

$$\Delta(C_1, C_2) = \sum_{j=1}^2 \frac{1}{|C_j|} (\hat{\theta}_{C_j} - \hat{\theta}_P)^2 \quad (5)$$

However, performing the two-stage estimation of $\hat{\theta}_{C_1}$ and $\hat{\theta}_{C_2}$ for all possible splits is too computationally expensive. Instead, we will approximate these estimates by taking a Newton Step from a parent node estimate $\hat{\theta}_P$. Let us first write the loss function of the second-stage residualized least square regression, $\mathcal{L}_{res}(\theta, Z_i) = \frac{1}{2} (\theta \tilde{T}_i - \tilde{Y}_i)^2$. Then for each observation Z_i that belongs to node P , the gradient is $\nabla_{\theta} \mathcal{L}_{res}(\hat{\theta}_P, Z_i) = (\tilde{Y}_i - \hat{\theta}_P \tilde{T}_i) \tilde{T}_i$. The empirical Hessian over the observations in

parent node P ,

$$A_P = \nabla_{\hat{\theta}}^2 \left(\frac{\sum_{i \in P \cap S_b^1} \mathcal{L}_{res}(\hat{\theta}_P, Z_i)}{|P \cap S_b^1|} \right) = - \frac{\sum_{i \in P \cap S_b^1} \tilde{T}_i^2}{|P \cap S_b^1|} \quad (6)$$

Then, for any child node C given by a candidate split, we could derive a proxy estimate $\tilde{\theta}_C$ by taking a Newton step with data in node C ,

$$\tilde{\theta}_C = \hat{\theta}_P - \sum_{i \in C} A_P^{-1} (\tilde{Y}_i - \hat{\theta}_P \tilde{T}_i) \tilde{T}_i \quad (7)$$

Given the estimates $\tilde{\theta}_C$, we compute the proxy heterogeneity score:

$$\tilde{\Delta}(C_1, C_2) = \sum_{j=1}^2 \frac{1}{|C_j|} (\tilde{\theta}_{C_j} - \hat{\theta}_P)^2 \quad (8)$$

We grow the tree by greedily selecting the splits that maximize this proxy heterogeneity score, until certain stopping condition is met. After the tree is grown, the set of observations in S_b^2 is “pushed down” to determine which leaf it falls in, while the learner ensures that the leaf contains at least r observations in S_b^2 . For each tree indexed $b \in [B]$, let $L_b(x)$ be the set of training example falling in the same “leaf” as the test point x . Then, the tree weight assigned to each observation i is computed as

$$K(X_i, x, (S_b^1, S_b^2)) = \frac{1[(X_i \in L_b(x)) \wedge (Z_i \in S_b^2)]}{|L_b(x) \cap S_b^2|} \quad (9)$$

Finally, we assign the importance weight for each observation by averaging over all the B trees:

$$K(X_i, x) = \frac{1}{B} \sum_{b=1}^B K(X_i, x, (S_b^1, S_b^2)) \quad (10)$$

For each observation, the importance weight measures the similarity between its feature vector(s) X_i and the target feature point x . It will be used for the next kernel two-stage estimation.

Weighted Two-Stage Estimation

We now describe how ORF uses the forest-based kernel learner to perform kernel estimation, which is summarized in Algorithm 3. The algorithm first partitions the input dataset D into D_1 and D_2 , and runs the forest-based weight learner on D_1 and D_2 to derive two forests and two sets of similarity weights. We use $\{\omega_{ib}\}_{b=1}^B$ and ω_i to denote the tree weights and importance weights over the observations in D_1 , and use $\{a_{id}\}_{d=1}^B$ and a_i to denote the tree weights and importance weights over the observations in D_2 . We will utilize these weights to perform a kernel two-stage estimation.

In the first stage, we pass the set of weights ω_i to observations in D_1 to estimate the local nuisance functions q_0 and g_0 at $X = x$, denoted as \hat{q} and \hat{g} . As suggested in Chernozhukov et al. (2017a), a broad array of sophisticated machine learning methods can be applied here, such as lasso, ridge, DNNs, random forests, and various hybrids and ensembles of these methods. Then, following the cross-fitting approach in DML, we compute the residualized \tilde{Y}_i and \tilde{T}_i for each observation $Z_i = (T_i, Y_i, W_i, X_i) \in D_2$: $\tilde{Y}_i = Y_i - \hat{q}(X_i, W_i)$, and $\tilde{T}_i = T_i - \hat{g}(X_i, W_i)$. We can obtain the estimates of $\theta_0(x)$ by performing a kernel linear regression over observations in D_2 :

$$\hat{\theta} = \arg \min_{\theta} \sum_{i: Z_i \in D_2} a_i (\theta \tilde{T}_i - \tilde{Y}_i)^2 \quad (11)$$

Note that GRF proposed in Athey, Tibshirani, and Wager (2019) also recommends such a residual on residual regression approach in their empirical study, which is referred to as “local centering,” albeit without theoretical analysis. The key difference between “local centering” and ORF is that ORF residualizes locally around test point x , as opposed to performing an overall residualization step and then calling the GRF algorithm on the residuals. Oprescu, Syrgkanis, and Wu (2018) have shown that ORF can better minimize non-local mean squared error and improve the final performance of the treatment effect estimates. The reason is that ORF requires that the nuisance estimator achieve a good estimation rate only around the target point x and residualizing locally seems more appropriate than running a global nuisance estimation, which would typically

minimize a non-local mean squared error. while it does add some extra computational cost as a separate first stage model needs to be fitted for each target test point.

SDNNs for Nuisance Estimation

Here we describe the underlying math when estimating the nuisance functions using SDNNs. Basically, we train the SDNNs by minimizing a loss function which is defined as weighted sum-of-square errors between the true value and model estimates. The weight a_i for each observation in D_1 is obtained by running the same tree learner over B random subsamples (without replacement). To mitigate overfitting, we employ weight decay using \mathcal{L}_2 regularization, a widely-used technique for regularizing neural network models. Therefore, we can estimate the nuisance functions by minimizing the loss function of our SDNNs defined in Equations (2):

$$\hat{q} = \arg \min_q \sum_{i \in D_1} a_i (Y_{it} - q_1(\mathcal{X}^P) - V_{it}^1 \Gamma^1)^2 + \lambda_q \|q\|^2 \quad (12)$$

$$\hat{g} = \arg \min_g \sum_{i \in D_1} a_i (T_{it} - g_1(\mathcal{X}^P) - V_{it}^1 \Gamma^1)^2 + \lambda_g \|g\|^2 \quad (13)$$

where, $\lambda \geq 0$ are the regularization parameters. Larger values tend to shrink the parameters in the parametric and nonparametric components toward zero.

Algorithm 1 Proposal Splitting Points

Input: d -dimensional feature space data X that are relevant at node P , number of selected features m , and number of proposal split points k

- 1: Randomly pick m columns of X , denoted as Z
 - 2: **for** each feature $j = 1, 2, \dots, m$ **do**
 - 3: Sort the possible value of Z_j , denoted as $V_j = \{v_1, v_2, \dots, v_N\}$
 - 4: Add $\min\{k, |V_j|\}$ randomly selected values from V_j to $Cand_p$
 - 5: candidate split points $Cand_p$ at node P
-

Algorithm 2 Gradient Tree (Forest-based Kernel Learner)

Input: tree splitting sample S_1 , estimation sample S_2 , minimum leaf size r , minimum ratio at each split ρ , maximum number of splits (tree depth) τ , number of randomly selected candidate features m at each split, and number of proposed split points k

- 1: Initialize the tree with root node P_0 covering the whole feature space, and the Queue $Q = \{P_0\}$
- 2: Initialize the observations belong to the current node P_0 as $S^{P_0} = \{S_1, S_2\}$
- 3: Initialize the accumulated number of splits $accSplits = 0$
- 4: **while** $NotNull(P \leftarrow Q)$ & $accSplits \leq \tau$ **do**
- 5: Perform the second-stage estimation of $\hat{\theta}_P$:

Estimate nuisance function \hat{q}_P and \hat{g}_P for observations in S_1^P ▷ See Web Appendix B

Calculate the residuals: $\tilde{Y}_i = Y_i - \hat{q}_P(X_i, W_i)$, $\tilde{T}_i = T_i - \hat{g}_P(X_i, W_i)$

Solve the optimization problem: $\hat{\theta}_P = \arg \min_{\theta} \frac{1}{|S_1^P|} \sum_{Z_i \in S_1^P} \frac{1}{2} (\theta \tilde{T}_i - \tilde{Y}_i)^2$

- 6: Compute the empirical Hessian: $A_P = -\sum_{i \in S_1^P} \tilde{T}_i^2 / |S_1^P|$
- 7: Generate k split points $Cand_P$ based on S_1^P ▷ See Algorithm 1
- 8: **for** each candidate split point $C \in Cand_P$ with children nodes C_1 and C_2 **do**
- 9: Obtain the remaining subsamples that belong to the children nodes, denoted as

$$S^{C_1} = \{S_1^{C_1}, S_2^{C_1}\}, \quad S^{C_2} = \{S_1^{C_2}, S_2^{C_2}\}$$

- 10: **if** $\min\{|S^{C_1}|, |S^{C_2}|\} \geq r$ & $\min\{|S_1^{C_1}|/|S_1|, |S_1^{C_2}|/|S_1|, |S_2^{C_1}|/|S_2|, |S_2^{C_2}|/|S_2|\} \geq \rho$ **then**
- 11: Compute the approximated estimates at each children node $j \in \{1, 2\}$:

$$\tilde{\theta}_{C_j} = \hat{\theta}_P - \sum_{i \in C_j} A_P^{-1} (\tilde{Y}_i - \hat{\theta}_P \tilde{T}_i) \tilde{T}_i$$

- 12: Compute the proxy heterogeneity score at node C :

$$\tilde{\Delta}(C_1, C_2) = \sum_{j=1}^2 \frac{1}{|C_j|} (\tilde{\theta}_{C_j} - \hat{\theta}_P)^2 = \sum_{j=1}^2 \frac{1}{|C_j|} \left(\sum_{i \in C} A_P^{-1} (\tilde{Y}_i - \hat{\theta}_P \tilde{T}_i) \tilde{T}_i \right)^2$$

- 13: **else**
- 14: Remove candidate C from the set $Cand_P$
- 15: **if** $NotNull(Cand_P)$ **then**
- 16: Select $C^* \in Cand_P$ that maximizes the proxy heterogeneity score
- 17: Update the sample S^{S_j} as these belong to the children node C_j^* for $j \in \{1, 2\}$
- 18: Update $\{C_1^*, C_2^*\} \leftarrow Q$, and $accSplits = accSplits + 1$

Output: tree T_{P_0} with root node P_0

Algorithm 3 Orthogonal Random Forests

Input: data set D of size N , target feature vector x , base tree learner \mathcal{L}_T , the number of trees B , subsamples size s , and minimum observation per leaf r

- 1: Randomly partition D into two data sets D_1 and D_2 of equal size
- 2: **procedure** NUISANCE ESTIMATION
- 3: **for** each tree $b \in 1, \dots, B$ **do**
- 4: Randomly sub-sample s observations from D_1 without replacement to form S_b
- 5: Randomly partition S_b into two datasets of even size: S_b^1 and S_b^2
- 6: Apply learner \mathcal{L}_T to build a tree T_b using $Z \in S_b^1$ and $X \in S_b^2$ \triangleright See Algorithm 2
- 7: Obtain the leaf $L_b(x) \subseteq \mathcal{X}$ that contains the target feature x
- 8: **for** each observation $i \in D_1$ **do**
- 9: Compute the tree weight: $\omega_{ib} = \frac{1[(X_i \in L_b(x)) \wedge (Z_i \in S_b^2)]}{|L_b(x) \cap S_b^2|}$
- 10: **for** each observation i in D_1 **do**
- 11: Compute the importance weight: $\omega_i = \frac{1}{B} \sum_{b=1}^B \omega_{ib}$
- 12: Estimate \hat{q} and \hat{g} using observations in D_1 and weights ω \triangleright See Web Appendix B
- 13: **procedure** TARGET ESTIMATION
- 14: **for** each tree $d \in 1, \dots, B$ **do**
- 15: Randomly sub-sample s observations from D_2 without replacement to form J_b
- 16: Randomly partition J_b into two datasets of even size: J_d^1 and J_d^2
- 17: Apply learner \mathcal{L}_T to build a tree T_d using $Z \in J_d^1$ and $X \in J_d^2$ \triangleright See Algorithm 2
- 18: Obtain the leaf $L_d(x) \subseteq \mathcal{X}$ that contains the target feature x
- 19: **for** each observation $i \in D_2$ **do**
- 20: Compute the tree weight: $a_{id} = \frac{1[(X_i \in L_d(x)) \wedge (Z_i \in J_d^2)]}{|L_d(x) \cap J_d^2|}$
- 21: **for** each observation i in D_2 **do**
- 22: Compute the importance weight: $a_i = \frac{1}{B} \sum_{d=1}^B a_{id}$
- 23: Compute the residuals: $\tilde{Y}_i = Y_i - \hat{q}(X_i, W_i)$, and $\tilde{T}_i = T_i - \hat{g}(X_i, W_i)$
- 24: Estimate $\hat{\theta}$ by solving the kernel residualized regression problem

$$\hat{\theta} = \arg \min_{\theta} \sum_{i: Z_i \in D_2} a_i (\theta \tilde{T}_i - \tilde{Y}_i)^2 \quad (14)$$

Output: The conditional average treatment effect $\hat{\theta}(x)$ at x

B. ENABLING SDNNS IN ORF

A team of researchers at Microsoft Research developed a Python package, *EconML*, for applying machine learning and causal inference method.¹ *EconML* contains a module for implementing ORF, built on the *sklearn* library for performing nuisance estimation. *sklearn* provides a wide range of parametric and nonparametric methods, such as lasso and standard neural networks architecture, but it doesn't allow both simultaneously. That is, one can implement ORF using package *EconML*, only when the nuisance function is assumed to be either completely parametric or having standard neural network architecture. In addressing this limitation, we contribute a PyTorch extension to the ORF library. In this appendix, we describe step-by-step how to build SDNNs in Python, followed by how to enable SDNNs in ORF using Python.

Among many libraries that can be used for deep learning, we adopt PyTorch, primarily developed by Facebook's AI Research lab, that offers much flexibility to construct neural network models using built-in functions and classes. We recommend installing PyTorch with Python 3.6 or greater. One will also need to install Skorch, a Python-based library for PyTorch that provides full Skicit-Learn (sklearn) compatibility.² The clean sklearn interface offered by Skorch could largely simplify the model training and evaluation process.

Our SDNNs is customized specifically to estimate the nuisance function g_0 and q_0 that capture the confounding effects of covariates on price and demand, respectively. It has two sets of input variables, χ^p and χ^n , which enter the parametric and nonparametric components of the model respectively. This requires a multiple-input feedforward neural network that takes χ^n and χ^p in separate branches and let only χ^n go through the nonlinear operations. The full code for building and training this SDNNs is provided in below. We explain each block in the following sections. For researchers and practitioners, it is easy to extend this semi-parametric framework and customize

¹See <https://econml.azurewebsites.net/spec/spec.html> for detailed documentation.

²For installation of PyTorch, see <https://pytorch.org/get-started/locally/>. For installation of Skorch, see <https://skorch.readthedocs.io/en/latest/index.html>. See [Skorch API documentation](#) for a complete list of arguments and methods. Skicit-Learn is an open source Python library that implements a wide range of machine learning using a unified interface. It is by far the easiest and most widely-used tools for machine learning applications.

their own DNNs by harnessing the full power of PyTorch.

```
import numpy as np
from torch import nn
import torch.nn.functional as F

from skorch import NeuralNetRegressor

X = torch.from_numpy(X).float()
Y = torch.from_numpy(Y).float()

class MyModule(torch.nn.Module):
    def __init__(self):
        super(RegressorModule, self).__init__()
        self.dense0 = nn.Linear(260, 100)
        self.dense1 = nn.Linear(100, 100)
        self.output = nn.Linear(100 + 1458, 1)

    def forward(self, X, **kwargs):
        X1, X2 = X[:, :260], X[:, 260:]
        X1 = F.relu(self.dense0(X1), inplace=True)
        X1 = F.relu(self.dense1(X1), inplace=True)
        X = torch.cat([X1, X2], 1)
        X = self.output(X)
        return X

net = NeuralNetRegressor(
    module=MyModule,
    criterion = torch.nn.MSELoss,
    optimizer = torch.optim.Adam,
    lr = 0.001
    # Shuffle training data on each epoch
    iterator_train__shuffle=True,
)
net.fit(X, Y)
y_pred = net.predict(X)
```

Data Preparation

Before building a model, we need to convert the input(s) and target(s) to PyTorch variables. PyTorch uses tensor to store and operate on n-dimensional rectangular arrays of numbers, which are similar to NumPy arrays but can also be operated on GPU and provides automatic differentiation that efficiently computes the gradient w.r.t. some parameters. Suppose the input data X and target Y are in Numpy arrays, we could convert them to PyTorch tensors using the following code:

```
X = torch.from_numpy(X).float().to(device)
```

```
Y = torch.from_numpy(Y).float().to(device)
```

The command `.to(device)` send data to the chosen device (CPU or GPU).

Defining SDNNs

We now illustrate how to implement a SDNNs defined in Section *SDNNs for Nuisance Estimation* using PyTorch API. We first create a class for our own neural network `MyModule` by subclassing `torch.nn.Module`. The `torch.nn.Module` is the base class in PyTorch that contains the building blocks needed to create all sorts of neural network architectures. Through class inheritance, we are able to use all of the functionality of the `nn.Module` base class, but still need to define the hyperparameters (e.g., the number of layers and the number of nodes in each layer) for our own network.³ The actual code used to define our model looks like this:

```
import torch.nn as nn
import torch.nn.functional as F
class MyModule(nn.Module):
    def __init__(self):
        super(MyModule, self).__init__()
        self.dense0 = nn.Linear(242, 100)
        self.dense1 = nn.Linear(100, 100)
        self.output = nn.Linear(100 + 1458, 1)
```

In the first line of the class initialization (`def __init__(self):`), we have the required Python `super()` function, which created an instance of the base `nn.Module` class. The following three lines are where we create our fully connected layers, which are represented by the `nn.Linear` object, with the first argument being the number of input nodes in layer l and the second argument being the number of outputs. The first layer `dense0` takes 242 inputs (the dimensionality and the shape of input data must match) and produces 100 outputs, followed by a 100-dim to 100-dim hidden layer `dense1`. These two layers consist a branch that will be used to operate over the set of input variables χ^n . Then we have the top layer, which accepts the derived 100 nodes from the

³Note that it is mandatory to subclass `torch.nn.Module` when you create a class for your own network. The name of your customized class can be anything.

hidden layer `dense1` along with another set of input variables (corresponds to χ^p), and outputs a single value - the final predication.⁴

After setting up the “skeleton” of our network architecture, the next step is to define how the data flows through the network and performs the computation. We do this by defining a `forward()` method in our class. For the `forward()` method, we supply the input data `X`, a Tensor contains all of our input variables, as the primary arguments. In the first line of the `forward()` class, we split `X` into `X1` and `X2`, corresponding to χ^n and χ^p respectively in Equation (2). We then feed `X1` into our first layer `dense0` and apply the activation function ReLU to the nodes in this layer using `F.relu()`. It is important to note that each layer itself is simply a linear combination of inputs and nonlinearity is added via the activation function. The transformed value is reassigned to `X1` and continuously fed to the next layer `dense1`, followed by ReLU activation. The derived nodes from `dense1` will then be combined with the auxiliary input `X2` at the `output` layer to obtain our final prediction. Note that, without nonlinear activation attached, this top layer is simply a linear model in `X2` and the derived nodes. The auxiliary input `X2` thus falls into the linear component of the model.

```
def forward(self, X, **kwargs):
    X1, X2 = X[:, :242], X[:, 242:]
    X1 = F.relu(self.dense0(X1), inplace=True)
    X1 = F.relu(self.dense1(X1), inplace=True)
    X = torch.cat([X1, X2], 1)
    X = self.output(X)

    return X
```

Training SDNNs

Now it is time to train the neural network. The original training process in PyTorch requires a fit loop, which typically generates a lot boilerplate code and is incompatible with ORF package. To ease the training process, we leverage the sklearn compatibility provided by Skorch. Skorch offers

⁴The dimension of input in the first layer is 242, which equals the number of covariates that assume to have nonlinear relationships with treatment/outcome in Table 1 plus the 1-d target feature (e.g., the number of days to scheduled live day). The input in the top layer is the vector of 1,458 creator, category, and time fixed effects.

two main classes, `NeuralNetRegressor` and `NeuralNetClassifier` (for regression and classification tasks respectively) that wrap the PyTorch `Module` while providing an training/evaluation interface similar as `sklearn`. Since our analysis focuses on regression task, we pass our Pytorch model to `NeuralNetRegressor`, in conjunction with a PyTorch (-compatible) criterion such as the loss function and optimizer. A sample code is provided in below:

```
net = NeuralNetRegressor(
    module=MyModule,
    criterion=torch.nn.MSELoss,
    optimizer=torch.optim.Adam,
    lr=0.001, ... ,
)
net.fit(X, y)

y_pred = net.predict(X_test)
```

We can see that `NeuralNetRegressor` wraps the PyTorch `Module` in an `sklearn` interface. The argument `module` is where we pass our PyTorch `Module`. The argument `criterion` specifies the loss function and is set to PyTorch `MSELoss` by default when you use the `NeuralNetRegressor`. More arguments, such as the optimizer and learning rate, etc., can be specified as well. After defining relevant arguments and methods to the wrapper, we could call `fit()` and `predict()`, as with an `sklearn` estimator. To evaluate the neural network model, we could call `score()` method that returns the coefficient of determination R^2 of the prediction for regressors.

Execution

To accommodate and streamline customized neural network usage in ORF, we contribute to the main ORF library a PyTorch extension. Our extension module addresses two issues. First, since the main ORF module generally takes Numpy Arrays while neural networks need to be feed with PyTorch Tensors, we perform format transformation when data flowing through the network. Second, although the Skorch wrapper offers `fit` and `predict` that looks like `sklearn` API, it is not fully `sklearn`-compatible in terms of inputs and outputs dimensionality/shape. We hence reshape input/output flows and apply dimensionality check at each key algorithmic block to guarantee full

sklearn compatibility of the customized neural network. Note that Skorch `fit()` does not support passing `sample_weight` directly as arguments to `fit` calls. Instead, we can pass the `sample_weight` with `X` as a dictionary to the `forward` method and then define your own loss function in Skorch.

The ORF package provides a helper class `WeightedModelWrapper` that enables sample weights functionality, by wrapping any class that supports `fit` and `predict`. Below is an example code of applying the wrapper on SDNNs:

```
model_T_final=WeightedModelWrapper(  
    model_instance=NeuralNetRegressor(MyModule,  
    lr=0.001,  
    optimizer=torch.optim.Adam,  
    optimizer__weight_decay=0.0001),  
    sample_type="sampled")
```

The first argument `model_instance` is where we pass our Skorch (-wrapped) model that requires weights. The second argument `sample_type` specifies method for adding weights to the model. For nonlinear model (e.g., neural network and random forest), this argument should be set to `sampled` method, which samples the training set according to the normalized weights and creates a dataset larger than the original. Set this argument to `weighted` for linear regression models where the weights can be incorporated in the matrix multiplication.

After enabling sample weights functionality for our SDNNs, we could now run the full ORF algorithm using the example code below. Since our treatment (i.e., price) is continuous, we call the class `ContinuousTreatmentOrthoForest` to perform ORF estimator. In the first two lines of the class, we specify hyperparameters that controls the tree-growing procedure for the forest kernel learner, in line with description in Section A.1. The argument `n_trees` controls how many trees are grown in the random forest. Generally, obtaining high-quality confidence intervals requires growing a large number of trees. The `min_leaf_size` relates to the minimum size a leaf node is allowed to have. Given this parameter, if a node reaches too small of a size during splitting, it will not be split further. The maximum number of splits are specified in the `max_depth` argument. The `subsample_ratio` is a number in range $(0, 1]$ that controls the fraction of samples should be used

in growing each tree. As noted in the “honesty” criterion, the fractional subsample will be further split into halves.

```
from econml.ortho_forest import ContinuousTreatmentOrthoForest
from econml.ortho_forest import WeightedModelWrapper

# Specify hyperparameters
est = ContinuousTreatmentOrthoForest (

    n_trees=500, min_leaf_size=100,
    max_depth=20, subsample_ratio=0.5,

    model_T=NeuralNetRegressor(MyModule,
    optimizer=torch.optim.Adam,
    lr=0.001, optimizer__weight_decay=0.0001),

    model_Y=NeuralNetRegressor(MyModule,
    optimizer=torch.optim.Adam,
    lr=0.001, optimizer__weight_decay=0.0001),

    model_T_final=WeightedModelWrapper(NeuralNetRegressor(MyModule,
    optimizer=torch.optim.Adam, lr=0.001, optimizer__weight_decay=0.0001),
    sample_type="sampled")

    model_Y_final=WeightedModelWrapper(NeuralNetRegressor(MyModule,
    optimizer=torch.optim.Adam, lr=0.001, optimizer__weight_decay=0.0001),
    sample_type="sampled")

)

est.fit(Y, T, X, W)

# Specify test points on the target feature X (time distance to live day)
X_test = np.linspace(-14, 14, 29).reshape(-1, 1)
treatment_effects = est.const_marginal_effect(X_test)
```

The following two arguments `model_T` and `model_Y` (for treatment and outcome respectively) are where we pass our semi-parametric DNN to the random forest kernel learner. Note that `model_T` and `model_Y` are used to perform first-stage estimation when placing splits in the tree and no weights will be involved at this tree-growing stage. The next two arguments `model_T_final` and `model_Y_final` are where we pass the semi-parametric DNN that supports sample weights derived from the random forest kernel learner. After defining relevant arguments and method, we could call `fit()` to start training. The final treatment effects at every test points can be produced by calling `const_marginal_effect(X_test)`. One can generate confidence intervals to wrap

the derived estimates using bootstrap, which has been proven in theory to be asymptotically valid (Oprescu, Syrgkanis, and Wu 2018).

C. NUISANCE FUNCTIONS AND HYPER-PARAMETERS

Comparing Different Specifications of Nuisance Functions

To illustrate the potential gain of using SDNNs to specify nuisance functions relatively to the existing common approaches (i.e., lasso and standard DNNs), we compare their performance in fitting observed (log-transformed) price and demand along a few dimensions, respectively. The lasso includes all the covariates in Table 1 linearly in the nuisance functions. The DNNs is implemented with the MLPregressor provided in sklearn library, which has a similar architecture to the SDNNs but without the parametric component. We randomly split all the Live-day observations into a in-sample training data set (80%) and a out-sample testing data set (20%). We use grid search to tune the hyperparameters of each mode.

Table W1: Fitting Comparison across Methods

		In-Sample		Out-Sample		
Model		R ²	MSE	R ²	MSE	Time (secs)
Demand Equation	Lasso	0.694	0.500	0.689	0.502	211
	DNNs	0.807	0.315	0.818	0.294	567
	SDNNs	0.755	0.400	0.786	0.355	292
Price Equation	Lasso	0.783	0.093	0.784	0.092	391
	DNNs	0.997	0.002	0.994	0.002	528
	SDNNs	0.978	0.010	0.980	0.006	517

Table W1 reports the performance comparisons. One can see that the neural network-based methods achieve much higher prediction accuracy than lasso in both demand and price equation. The out-sample R² and MSE both improve by at least 27%. This suggests that, as we expected, linear functional form cannot fully recover the complex relationships between the large number of covariates and price/demand. Within the two neural network models, DNNs achieve slightly higher prediction accuracy than SDNNs, but also involve higher computation costs. This is because SDNNs do not interact a large number of variables for capturing individual and time fixed effects with other covariates, while DNNs naively dump all covariates (including fixed effects) into the

neural network blackbox.

Parameterization in ORF

The random forest kernel learner requires us to select three tuning parameters: the number of trees, the minimum number of observations in each leaf, and the subsample size. In the absence of formal criteria to guide our choices, we used a large number of trees because more trees reduce the Monte Carlo error introduced by subsampling. We found moving from 100 to 500 improved the stability of estimates across samples, but moving from 500 to above does not improve stability significantly. Increasing the minimum number of observations in each leaf trades off bias and variance; bigger leaves make results more consistent across different samples but predict less heterogeneity. Smaller subsamples reduce dependency across trees but increase the variance of each estimate, though we find that increasing subsamples made little difference in our application (Davis and Heller 2017). Note that there is no formal rule to determine the number of test points. We choose these test points in order to obtain a reasonable tradeoff between granularity (of the estimates) and computational load.

D. PRICE COMPARISON ACROSS COMPARABLE LIVESTREAMING PLATFORMS

To the best of our knowledge, Zhihu Live is the largest livestreaming platform of its type during our study period. Its competing platforms were quite small during this period. We identify four relatively similar platforms in China that may compete with Zhihu Live. In summer 2016, we surveyed the prices of events on these five platforms, by randomly scraping 100 paid events on each platform. The descriptive statistics of these prices are shown in Table W2. To make sure that prices are comparable across platforms, we anchored the unit to RMB per 30min. We find that the price points for events hosted on Zhihu Live are typically higher than those of comparable events on competing platforms.

Table W2: Price Comparison

Platform	Mean	Median	Std. Dev.
Zhihu Live	12.81	13.82	9.50
Himalaya FM	5.95	4.06	5.56
Dedao	3.52	2.68	2.58
Lychee Live	12.87	4.95	29.43
Qianliao Live	3.36	2.91	3.01

E. SUPPLEMENTARY TO ORF ESTIMATION RESULTS

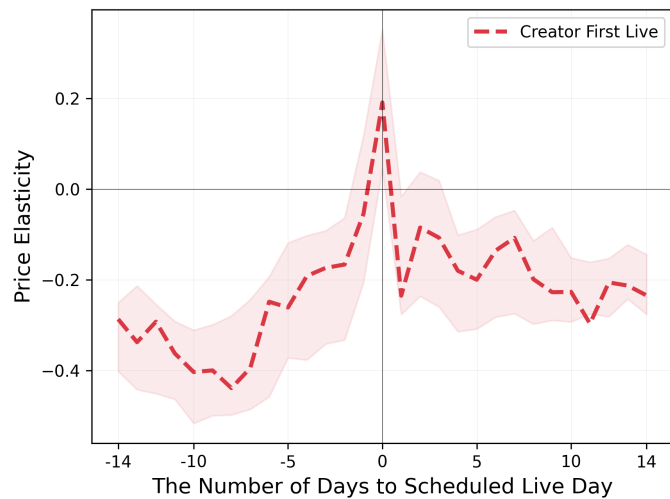


Figure W1: Price Elasticity over Time to Scheduled Live Day (Only the First Live per Creator)

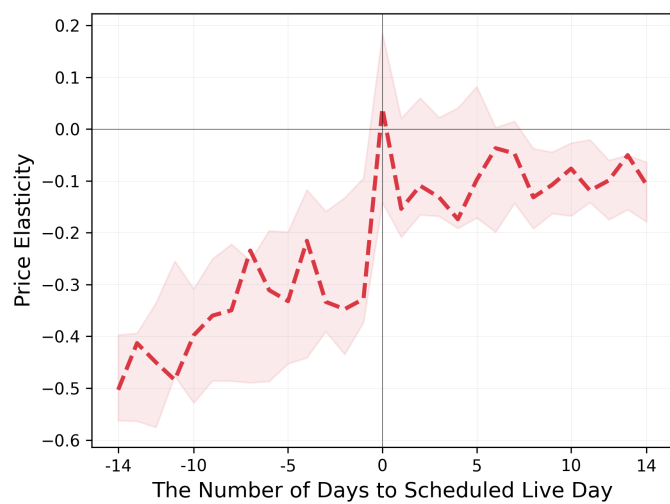


Figure W2: Price Elasticity over Time to Scheduled Live Day (Including the Interaction Terms of Creator Fixed Effects and Time Fixed Effects)

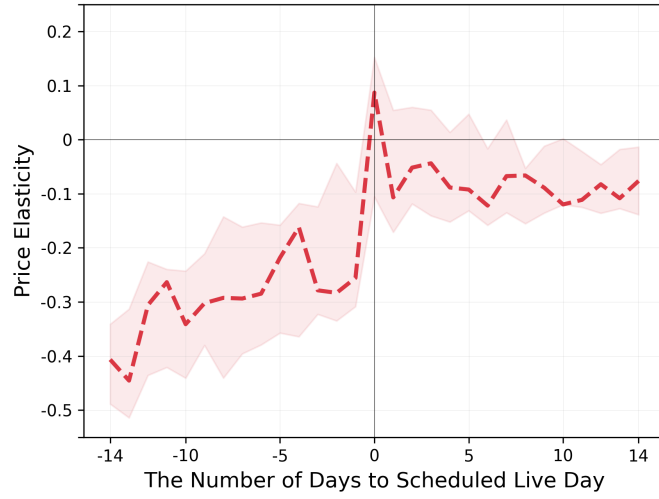


Figure W3: Price Elasticity over Time to Scheduled Live Day (Excluding Extreme Consumers)

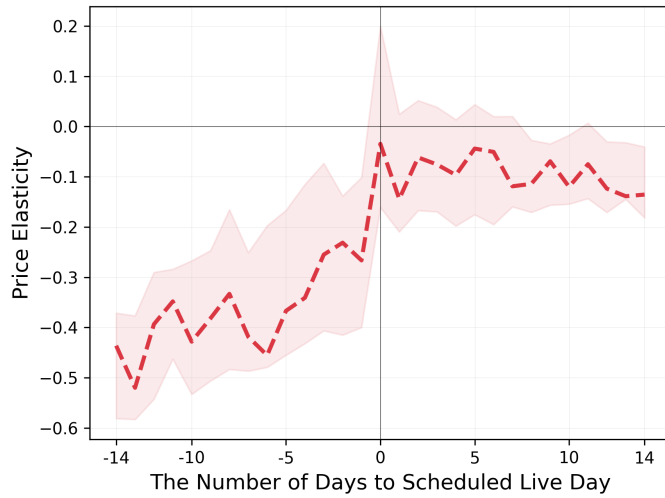


Figure W4: Price Elasticity over Time to Scheduled Live Day (Excluding Extremely Expensive Lives)

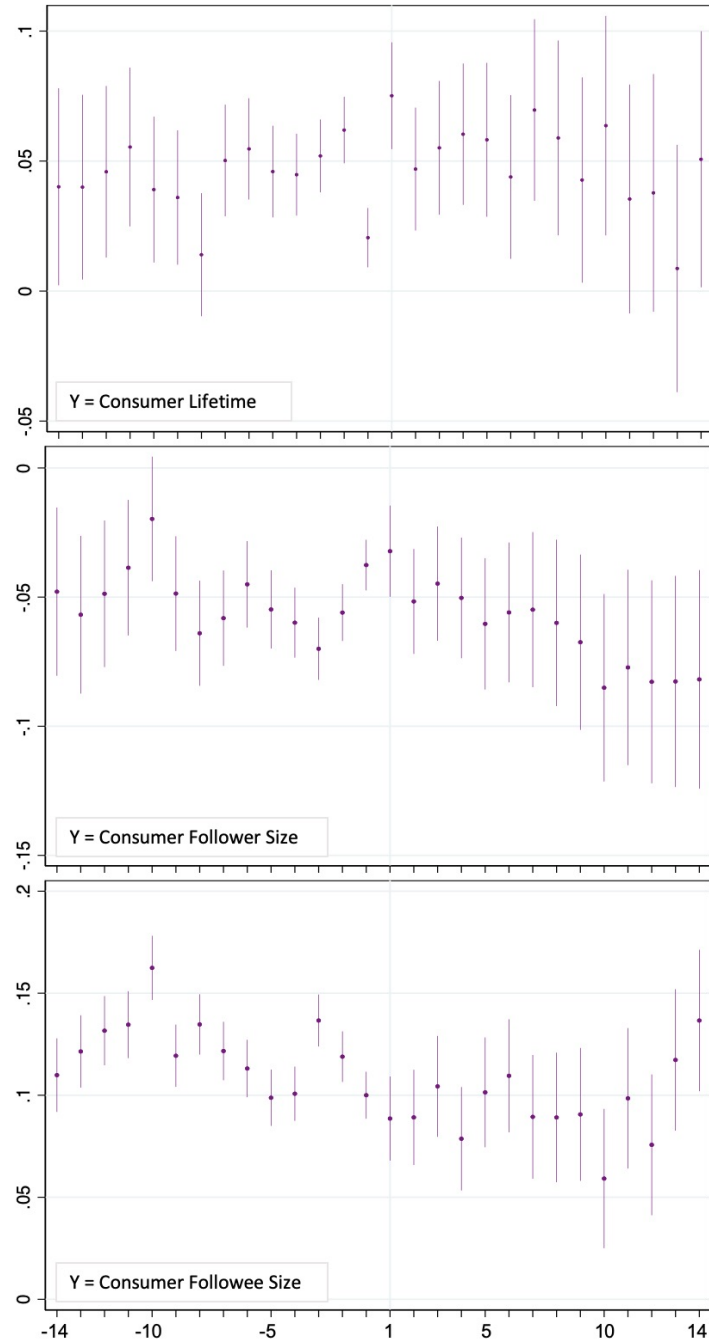


Figure W5: Variations in Consumer Characteristics over Live Life-Cycle

Note: The figures depict the estimated fixed effects of temporal distance to livestreaming day on three different consumer characteristics, along with the associated 95% confidence intervals.

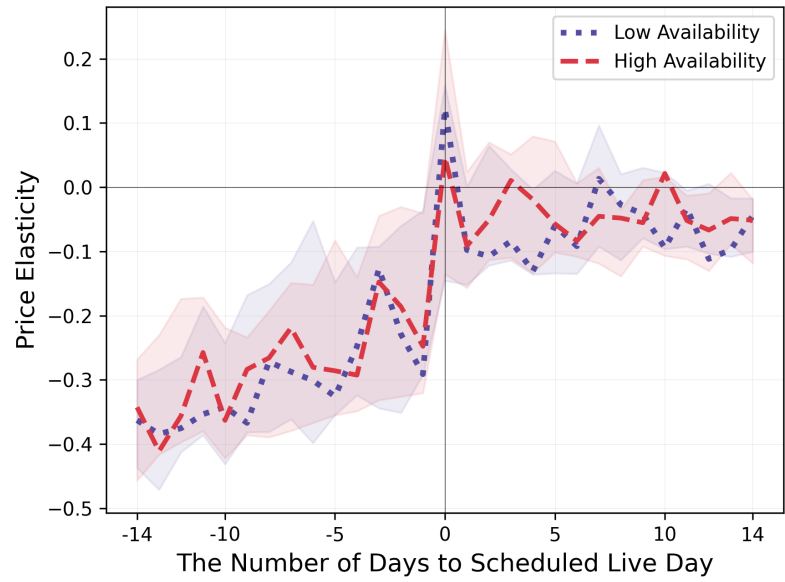


Figure W6: Price Elasticity and Consumer Availability

Note: The shaded region depicts 95% confidence interval via 100 bootstrap resamples.

F. IDENTIFICATION USING INSTRUMENTAL VARIABLES

Double Machine Learning with Instrumental Variables

Chernozhukov et al. (2018) propose a method for double machine learning estimation with instrumental variables, denoted by DMLIV. This method estimates the average treatment effect that solves the empirical analogue of the following moment equation:

$$\mathbb{E}[(Y - \mathbb{E}[Y|X, W] - \theta(T - \mathbb{E}[T|X, W]))(Z - \mathbb{E}[Z|X, W])] = 0,$$

where Y, T, X, W have the same definitions as in Equation (1) and Z is the instrumental variable. This moment function is orthogonal to all the first-stage functions $q_0(X) = \mathbb{E}[Y|X, W]$, $p_0(X) = \mathbb{E}[T|X, W]$ and $r_0(X) = \mathbb{E}[Z|X, W]$ that also need to be estimated from data. Thus, this method can be viewed as an extension of two-stage-least-squares (2SLS) approach to allow for arbitrary machine learning techniques to estimate the first stage functions $\hat{q}, \hat{r}, \hat{p}$ (Chernozhukov et al. 2020). This moment avoids the estimation of the expected T conditional on Z, X that satisfies an orthogonality condition that enables robustness of the estimate $\hat{\theta} = \frac{\mathbb{E}_n[(Y - \hat{q}(X, W))(Z - \hat{r}(X, W))]}{\mathbb{E}_n[(T - \hat{p}(X, W))(Z - \hat{r}(X, W))]}$, to errors in the nuisance estimates $\hat{q}, \hat{r}, \hat{p}$. The estimate is asymptotically normal with variance equal to the variance of the method if the estimates were the correct ones, assuming that the mean squared error of these estimates decays at least at rate of $n^{-1/4}$. See section 4.2 of Chernozhukov et al. (2018) for more details.

Analysis and Results

The main challenge of implementing DMLIV is to identify instrumental variables that correlate with creators' pricing decision (i.e., relevance condition) and affect demand only through price (i.e., exclusion restriction condition). As discussed in subsection *Other Identification Concerns and Robustness Checks*, we use two unique features of Lives as instruments: (1) the number of picture messages (e.g., prepared slides and photos) a creator sent in the Live chat room during the livestream, and (2) the average thumbs-up on messages posted by the creator. We find that our

proposed instrumental variables significantly affect price and also pass the weak instruments test ($F = 3,266, p < 0.05$).

Nevertheless, it is noteworthy that the validity of instruments, which depends on institutional setting and data generating process, is untestable. This is especially the case for the exclusion restriction condition, which assumes that the instrument should not affect the dependent variable (e.g., demand) directly, but only through the endogenous variable (e.g., price). This is analogous to the challenges in validating the unconfoundedness assumption in ORF or DML. The literature has suggested that the use of instruments that do not satisfy the key assumptions can result in more biased and misleading estimates (Sands 2018; Bound, Jaeger, and Baker 1995; Imbens 2014), and cautions must be taken when one relies on instrument variables for causal attribution.

Therefore, we compare the results from DMLIV and DML. If the instruments (and/or the unconfoundedness assumption) is invalid, the results from the DMLIV and DML are likely to be different. Table W3 compares the estimated average price elasticity in the pre- and post-period, respectively, using DML and DMLIV. We find similar point estimates between these two methods. In particular, their 95% confidence intervals overlap within each time period, though the confidence intervals based on DMLIV tend to be much wider.

Table W3: Comparing Estimated Price Elasticities

	<i>DML</i>	<i>DMLIV</i>
Pre-period	-0.205 (-0.235, -0.175)	-0.283 (-0.332, -0.233)
Post-period	-0.101 (-0.112, -0.090)	-0.115 (-0.136, -0.094)

Note: The 95% confidence intervals are in parentheses. The DML estimates in the pre-period (post-period) can be roughly interpreted as the average value of ORF estimates over test points $d \in [-14, 0]$ ($d \in (0, 14]$).